TITLE: **Light Hydrocarbon Gas Conversion Using Halogenated Iron Dodecaphenylporphyrin Catalysts**

PI (Authors): *M. Showalter, K. Erkkila, J. A. Shelnutt*

Institution/Organization: Fuel Science Department 6211
Sandia National Laboratories
Albuquerque, NM 87185

Contract Number: FEW-4262

Period of Performance: FY92-FY93

Objective: Use computer-aided molecular design techniques to develop new catalysts for conversion of light hydrocarbon gases to liquid fuels.

Accomplishments & Conclusions:

We are using computer-aided molecular design (CAMD) methods to engineer catalysts for light hydrocarbon-oxidation reactions. The objective is to enhance activity and selectivity of the reaction by developing a new generation of catalysts. Analysis of naturally occurring enzymes that catalyze light hydrocarbon oxidation (cytochrome P_{450}) and other small molecule reactions (carbonic anhydrase) has identified several structural features that are required to mimic the enzyme's high activity and selectivity using a synthetic analog of the enzyme. These include (1) a metal center with the suitable coordinated molecular groups and promoters and (2) a "rigid" binding cavity of the size and shape of the alkane molecule to be converted. These structural features have now been designed into catalysts derived from the class of dodeca-substituted porphyrins.

We are using this biomimetic approach to develop a process for the direct conversion of methane to methanol. Of several biomimetic alkane-activation chemistries presently known, the most interesting reaction for methane conversion is the one that uses a liquid/gas phase reaction based on a porphyrin catalyst and O_2 as the oxidant. The advantage is that no co-reductant is required to activate oxygen for this air-oxidation process. Our biomimetic computer-aided design approach is improving the specificity and reactivity of the catalysts used by this process for oxidation of light hydrocarbon gases. This is accomplished first by providing a shape selective cavity adjacent to the porphyrinic metal center at which the reaction takes place. Among other advantages, the cavity can determine the region of the hydrocarbon at which oxidation takes place, and, more importantly, may influence the product slate and catalytic rates by trapping of radical intermediates thought to be involved in the reaction. With regard to the latter, the autooxidation occurring in this reaction proceeds by a mechanism different from the biological reaction which gives only alcohols. Trapping of free radical intermediates is one possible mechanism by which the P_{450} enzyme may select specific oxidation products (alcohols) over other species. Reactions occurring in the "micro-reactor" environment of the cavity of our synthetic enzyme analogs can enhance catalytic activity and product selectivity in the process.

Metalloporphyrins and other metal containing heterogeneous materials catalyze the oxidation of light alkanes with air or oxygen as oxidant under mild conditions with no added co-reductant. (Figure 1. Ellis, Jr., P. E.; Lyons, J. E., Symp. Oxygen Activation in Catalysis, ACS, April 22-27, 1990. European Patent Appl. No. 88304455.4, 1988.) Prior work has indicated three beneficial properties that are desired of the metalloporphyrin catalysts. These activity-enhancing features are: **(1)** the presence of strongly electron-withdrawing substituent groups at the periphery of the porphyrin ring, **(2)** an axial ligand complex favoring the most negative Fe(III)/Fe(II) redox potential, and **(3)** steric restraints on close bimolecular face-to-face approach of catalyst molecules (Nappa, M. J.; Tolman, C. A., *Inorg. Chem.* **1985**, 24, 4711).

We have designed, synthesized, and tested a series of catalysts, based on the dodecaphenylporphyrins (DPPs), with enhanced features **(1)** and **(3)**, and with addition of a fourth feature--**(4)** a shape and size selective cavity that promotes the binding of the substrate alkane molecule. The cavity should favor binding of light hydrocarbons (methane, ethane, n-propane, and n-butane) over the alcohol product. Binding of the light hydrocarbon will increase activity by increasing the residence times of the substrate at the catalytic metal site. Selectivity for the alcohol can be improved by cage trapping and recombination of any radical intermediates in the reaction and by ejection of the alcohol product before further oxidation of the alcohol can occur. We have used computer-aided molecular design to engineer a class of catalysts, the halogenated-DPPs, with improved features **(1)**, **(3)** and **(4)**.

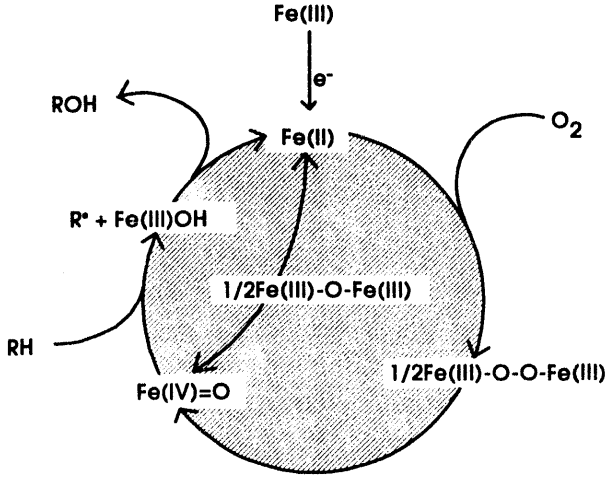

Figure 1. Proposed mechanism for oxidation of light hydrocarbons by Fe porphyrin catalysts.

Catalysts with Electron Withdrawing Peripheral Substituents. We and others have shown that electron withdrawing substituents at the periphery of the iron porphyrin catalyst have at least two beneficial effects. First, such substituents may activate the high oxidation state metal-oxo intermediate and increase its reactivity. Second, by removing electron density from the porphyrin ring, the substituents make the porphyrin less susceptible to self-destruction by electrophilic attack by the oxo intermediate of the catalyst. Table 1 shows the effect of increasing electron withdrawal by the substituents on the catalyst turnover rate for a series of halogenated Fe(III)

tetraphenylporphyrin (TPP) derivatives studied by Ellis and Lyons. We have used the Hammett σ values as a measure of the electron withdrawing capability of the individual substituent and summed these for the total electron withdrawal for each porphyrin. The data in Table 1 shows that the activity of the catalysts follows the degree of electron withdrawing ability of the substituents ($\Sigma\sigma_p$). A steric effect may also be evident for $MTPPCl_8$ derivatives (*vide infra*).

Table 1. ***Effect of Electron Withdrawal by Substituents on Catalyst Activity in Isobutane Oxidation.***

Catalyst	Turnover/hour[a]	$\Sigma\sigma_m$	$\Sigma\sigma_p$	Selectivity to TBA[b], %
FeTPP(Cl)	0	0.24	-0.04	-
$FeTPP\beta\text{-}Br_4(Cl)$	26	1.56	0.92	-
$FeTPPCl_8(Cl)$	43	0.4-0.8	0.4-0.8	89
$FeTPPCl_8\beta\text{-}Br_4(Cl)$	144	2.0-2.4	1.3-1.7	83
$FeTPPF_{20}(Cl)$	340	1.36	1.64	90

a. Turnover = moles O_2 consumed/mole catalyst. b. moles *t*-butylalcohol/total moles liquid product.

We have designed, synthesized and tested a series of new catalysts, the halogenated dodeca-substituted porphyrins (e. g., $DPPF_x$, x=0, 20, 28, 36, shown in Figure 13). (Figure 13 also lists the sums of the Hammett σ's of the substituents for these catalysts.) Clearly, the predicted electron depletion from the porphyrin ring ranges from about that of the catalysts used in the Sun work to about twice as great. Thus, the more electron depleted porphyrins like $FeDPPF_{36}$ can be expected to exhibit enhanced activity over prior catalysts. Further, the high depletion of charge density in the porphyrin ring of the halogenated catalysts also makes them more stable to electrophilic attack and self-destruction.

Steric Constraints on Bimolecular Interactions. Past work has shown that bulky substituents attached to the porphyrin which prevent close face-to-face approach of two porphyrins increase the resistance of the porphyrin to bimolecular destruction. The proposed new catalysts have this advantage as well. Because of the steric crowding of substituents at the periphery, the porphyrin macrocycle is distorted in such a fashion that the β-pyrrole substituents are oriented in a quasi-axial direction. The result is considerable steric hinderance in the face-to-face approach of two porphyrin macrocycles. For example, for the $FeDPPF_x$ catalysts, edge-on phenyl groups block close approach at each face of the porphyrin.

The steric constraints on face-to-face interactions of the porphyrins may also play a beneficial role in the reaction mechanism illustrated in Figure 1. In the proposed mechanism, adventitious impurity or the alkane itself reduces Fe to start the catalytic cycle. Then a peroxo-bridged dimer is formed and splits to give the reactive Fe(IV)=O intermediate. This ferryl intermediate subsequently reacts with the alkane (RH) to form the alcohol (ROH). A competing reaction of the intermediate is the formation of μ-oxo porphyrin dimer (Fe(III)-O-Fe(III)). The μ-oxo dimer is unreactive with the alkane. Thus, steric hinderance of the formation of face-to-face μ-oxo dimer is desirable, but formation of the peroxo dimer must still be favorable.

Molecular modeling indicates that this is the case for the $FeDPPF_X$ catalysts as shown in Figure 2. As a consequence, we expect the activity to be enhanced by favoring formation of the peroxo dimer over the μ-oxo dimer. The peroxo dimer may also be strained which could aid in the formation of the active ferryl (oxo) intermediate thus further enhancing catalytic activity. Another possible mechanism is based on formation of an alkyl hydroperoxide intermediate as proposed by Paulson *et al.* in 1974 (Paulson, D. R.; Ullman, R.; Soane, R. B.; Closs, G. L., *J. Chem. Soc., Chem. Commun.* **1974**, 186).

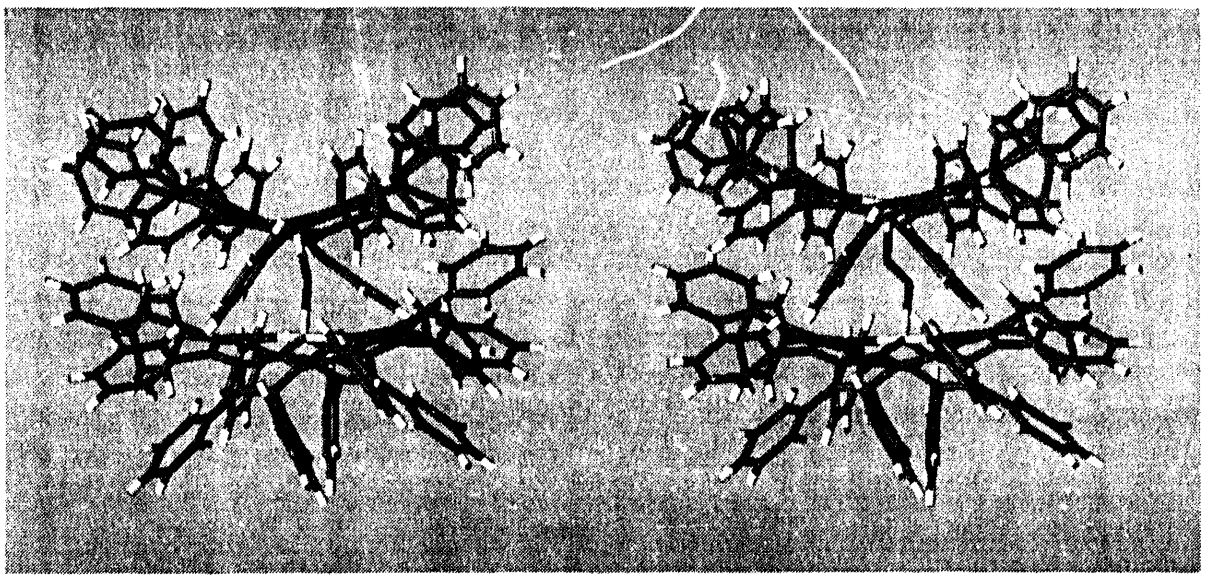

Figure 2. *Calculated structures of the μ-oxo- (left) and μ-peroxo- (right) dimers of the halogenated Fe dodecaphenylporphyrin. Calculated energies predict that the* active *peroxo-dimer intermediate is energetically favored, but the* inactive *oxo-dimer is unfavored by greater than 50 kcal/mol.*

Substrate Binding Cavity. Molecular modeling studies show that the new $FeDPPF_X$ catalysts have a cavity formed by the porphyrin ring and the quasi-axial CH's and CF's of the phenyl substituents. The cavity is of the size and shape of small linear alkanes (C_n, $n<4$). Energy minimization and molecular dynamics calculations show that methane will bind to the cavity and remain for significant times even in a vacuum at temperatures up to and above room temperature. Substrate binding is partly a consequence of the rigidity of the binding cavity and the favorable electrostatic interaction between the light hydrocarbon and the fluorocarbon groups of the cavity. The cavity is even more rigid than the earlier, first generation octaalkyl-tetraphenylporphyrin (OATPP) catalysts. As a consequence of the presence of a light hydrocarbon binding cavity we expect enhanced catalytic activity as a result of an increase of the residence time for the substrate at the active metal site in gas phase reactions. Radical trapping of the intermediates R• and •OH in the cavity may also promote recombination to form the alcohol product, thereby enhancing selectivity. Finally, ejection of the product upon its formation is expected as a result of the repulsion of the alcohol oxygen atom by the fluorine atoms lining the pocket. This repulsive interaction between the product and the substrate binding cavity serves two purposes. First, it clears the cavity after the reaction has occurred for the next alkane molecule to enter, and,

second, it prevents further oxidation of the alcohol molecule formed. The former effect is expected to result in higher catalytic rates; the latter is expected to improve selectivity for alcohol versus other oxidation products (ketones, aldehydes).

Synthesis of Advanced Catalyst Designs for Light hydrocarbon Activation. The halogenated dodeca-substituted porphyrins $DPPF_{20}$ (see below, Figure 13) represent the second generation of designed catalysts. To date, we have completed the synthesis of the free bases H_2DPPF_x, with x = 0, 20, 28, and 36. The Fe(III)Cl derivatives of all of these porphyrins have been synthesized and tested.

Many other catalysts with even higher electron withdrawing potentials have been designed and are currently being synthesized. We have now focused our synthesis work on potentially more active catalysts, the octaphenyl-tetranitro porphyrins (OPTNPs), which possess much higher ring electron depletion. (Some of new catalysts are shown in Figure 10 in the next section.) The first of these, OPP, has already been synthesized in quantities suitable for tests and iron is now being inserted. The synthesis of the tetra-nitroOPP [$(P)_8(NO_2)_4P$] has been completed in low yield and the porphyrin synthesis reaction is being optimized. This catalyst has the highest electron depletion ($\Sigma\sigma_m = 3.32$) of the catalysts synthesized so far. We anticipate no problems in progressing to the Fe(p-ClP)$_8$(NO$_2$)$_4$P and Fe(p-NO$_2$P)$_8$(NO$_2$)$_4$P catalysts with even higher macrocycle electron depletion (Figure 10), since one of the required pyrroles has already been synthesized.

One problem that is beginning to hinder the use of our designed catalysts is their low solubility in many organic solvents. To solve this problem we have designed more soluble analogs. For example, OPP has poor solubility, but by adding p-isopropyl groups to the phenyl substituents we obtain the highly soluble O(*p*-isopropylP)P analog (Figure 11). The synthesis of this catalyst is about half complete currently. After completion O(*p*-isopropylP)P will be nitrated and Fe incorporated to give Fe(III)O(*p*-isopropylP)TNP, a catalyst with both high solubility and strong electron depletion. The fluorinated isopropyl group could also be used to increase solubility and further increase electron depletion of the porphyrin macrocycle.

We have also synthesized additional Fe octaethyl-tetranitroporphyrin, a catalyst originally provided by Prof. Martin Quirke at Florida International University. The highly electron-withdrawing nitro groups potentially make the Fe derivative of this catalyst both highly catalytically active and oxidatively stable.

Finally, we have synthesized an alkane soluble porphyrin (Figure 12), thus, removing the necessity of a solvent other than the alkane to be oxidized and providing a means to support the catalyst on heterogeneous substrates.

Testing for Catalytic Activity of the Designed Catalysts. We now have succeeded in testing the second generation of designed catalysts for light alkane conversion. Our activity tests for the first-generation nonfluorinated OATPP catalysts are now completed and served to identify the direction we have subsequently followed in the design of more active catalysts. Current activity testing is focused on the halogenated Fe(III) dodecaphenylporphyrins ($FeDPPF_X$) using the iodosylbenzene shunt reaction (*vide infra*). We plan to re-test all of these designed catalysts in methane and isopentane oxidation using air or O_2 as the oxidant now that quantitatively reliable results have been obtained using the teflon-lined reactor shown in Figure 3. Isopentane is a useful substrate for our tests because it provides selectivity information for primary, secondary, and tertiary alcohols, and the primary alcohol information can be used to infer methane oxidation results. The selectivity data provide information about the effectiveness of the designed cavity.

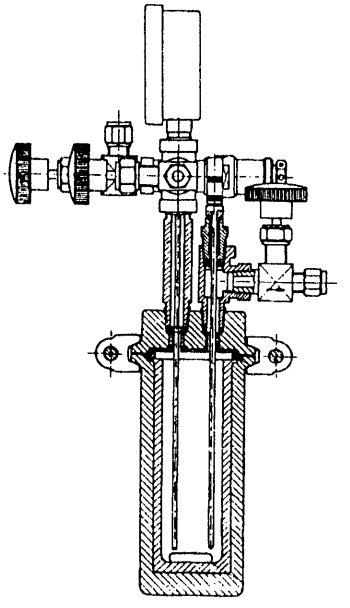

Figure 3. *New Berghof/America teflon-lined reactor shown without temperature controller and mantle.*

We have used the air/O_2 partial oxidation reaction to oxidize isopentane in the new teflon-lined reactor (Figure 3). The reaction conditions we used were 600 psig O_2 at 120 °C for 5 hours. The solvent used was benzene (5 ml) with [illegible]e added at a concentration of 2 M. The catalyst was $FeTPPF_{20}$. The catalytic rate a[illegible]ver the run was initially very low compared with previous reactions in the stainless ste[illegible]tor. We have now investigated the cause of the low yield, and, very recently we have obtained high yields in the teflon reactor. Sufficient reproducibility in the new reactor has now been obtained so that accurate comparison of measured catalytic rates are possible.

Figure 4 shows the effect of catalyst concentration on apparent catalytic activity in 6-hour runs. Similar, curves are noted for the iodosylbenzene reaction. In both cases the curves are a consequence of the low concentration of oxidant in the reaction solution. Obviously, the reaction conditions need to be optimized before true activities of the catalysts can be measured.

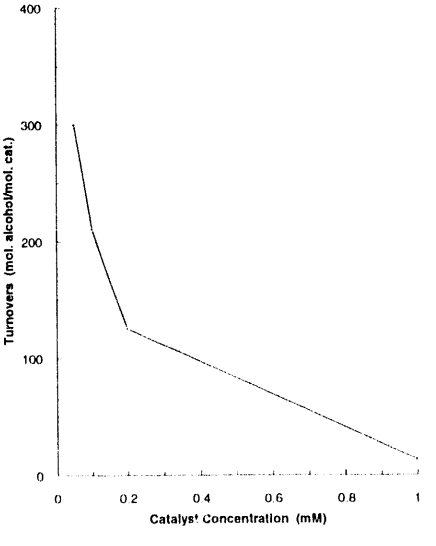

Figure 4. *Catalyst turnovers in 6 hours as a function of catalyst concentration.*

Apparent activities of the $FeDPPF_X$ catalysts at 50 μM concentration have been measured at 20 atmospheres O_2 and 100° C in benzene with isopentane as the substrate. The activities are plotted in Figure 5 as a function of the sum of the Hammett constants of the substituents on the

porphyrin. A good correlation between the electron-withdrawing capacity of the substituents and activity is found. Now that reliable activity measurements are possible with the O_2 partial oxidation reaction we will primarily use this test.

Meanwhile, we have continued to test the catalysts using the iodosylbenzene reaction and isopentane as the substrate. Although the primary focus of the research is methane partial oxidation, at the present stage of catalyst development the isopentane experiments are completely adequate to predict the activity of the catalysts in methane oxidation. Methane activity can be accurately estimated based on overall alcohol production and the known CH bond strengths of tertiary, secondary, and primary alkanes relative to the CH bonds of methane. None of the catalysts studied to date are competitive with high temperature partial oxidation reactions for methane as the substrate at the present stage of development, so little is to be gained by methane studies at this stage. On the contrary, isopentane oxidation provides much needed information about the reaction environment in the substrate binding cavity. This structural and mechanistic information is needed to further improve the catalysts.

In the iodosylbenzene reaction we expected to see low turnovers for the first generation of designed catalysts-the FeOATPPs. This is because the electronic effect on overall yield is adversely affected by the electron-donating groups that form the pocket for the substrate. For the designed catalysts, a similar relationship was observed with the catalytic activity increasing by over a factor of ten as the electron depletion of the macrocycle increases. The second generation of catalyst, the DPPs, were designed with strong electron-withdrawing groups instead of the alkyl substituents to correct this deficiency.

Catalytic activity testing focused on the halogenated dodeca-substituted iron porphyrins. The series of $FeDPPF_X$ (x=0, 20, 28, 36) catalysts

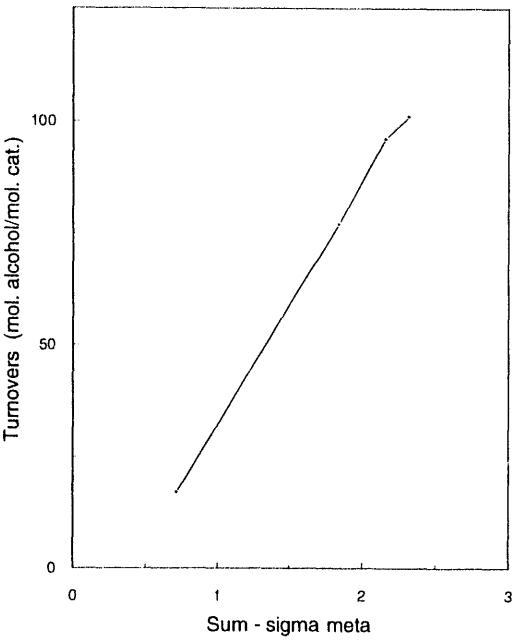

Figure 5. *Catalytic activity as a function of electron-withdrawing capacity of the substituents for the $FeDPPF_X$ series.*

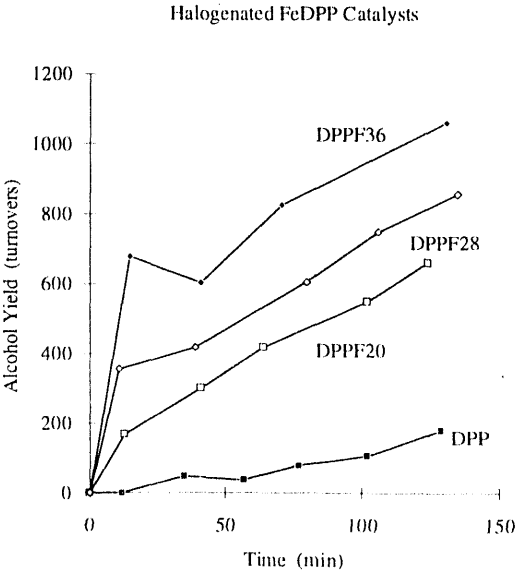

Figure 6. *Typical alcohol yields in catalyst turnovers as a function of reaction time. Catalyst concentration is 0.001 mM. The reaction slows after about 1 hour because the oxidant is depleted.*

provide novel selectivity and high stability and activity, giving catalytic rates of well over 2500 turnover/hr (moles alcohol product/moles catalyst/hr) in the iodosylbenzene shunt reaction. The catalysts tested from the fluorinated FeDPP series (Figure 13), include $DPPF_{20}$, $DPPF_{28}$, $mDPPF_{36}$. Un-fluorinated FeDPP, while not expected to be particularly active, was also synthesized to complete the series and was useful for the determination of structure-activity relationships and future design goals. The Fe(III)Cl derivative of tetra(pentafluorophenyl)porphyrin ($FeTPPF_{20}$) was tested for reference with other catalytic rate measurements.

The fluorinated FeDPP catalysts represent the first of the second generation of catalysts. The most important new testing results for the $FeDPPF_x$ (x=0, 20, 28, 36) catalysts are shown in Figure 6. These new tests include the complete $FeDPPF_x$ series for the first time and were run under conditions closer to the region of linear dependence on catalyst concentration than previous tests. The designed catalysts show a trend of increasing activity with increasing electron-withdrawing ability of the porphyrin substituents ($\Sigma\sigma_m$). Based on the sum of the meta Hammett constants σ_m, the electron-withdrawing ability of the phenyl and fluorophenyl substituents of FeDPP, $FeDPPF_{20}$, $FeDPPF_{28}$, and $FeDPPF_{36}$ are 0.72, 1.84, 2.16, and 2.96, respectively (Figure13). The activities of 0.001-mM solutions of the fluorinated DPPs are shown in Figure 6 and the initial catalytic rates are plotted in Figure 7. Adding more fluorines to FeDPP clearly results in increased activity as expected on the basis of the increasing electron-withdrawing effect. The high activity of $FeDPPF_x$ catalysts is a result of (1) substrate binding to the cavity, (2) selective oxidation of the substrate rather than oxidant, (3) a nonplanar distortion effect on iron activity, (4) prevention of μ-oxo dimer formation, and (5) dependence of activity on electron-depletion of the porphyrin ring.

The effect of the electron withdrawing capacity of the substituents on the catalytic rates of alcohol production is illustrated in Figure 7, where the rates are plotted versus $\Sigma\sigma_m$. A good linear correlation is observed. This clearly demonstrates the desirability of synthesizing porphyrins with even higher porphyrin ring electron depletion.

Recent tests with $FeDPPF_{20}$, for which the electron withdrawing capacity of the substituents is almost the same as $FeTPPF_{20}$ ($\Sigma\sigma_p$ = 1.56 vs. 1.64 for $FeTPPF_{20}$), indicate that the activity of $FeDPPF_{20}$ is about 50% greater than for $FeTPPF_{20}$. The higher activity of $FeDPPF_{20}$ is probably a result of steric hinderance in the formation of the μ-oxo dimer. We have modeled additional target catalyst designs with electron-withdrawing constants ($\Sigma\sigma_p$) of up to 7.3; those catalysts tested so far have electron-withdrawal of up to 2.8 only. Clearly, significant improvements in activity can be expected.

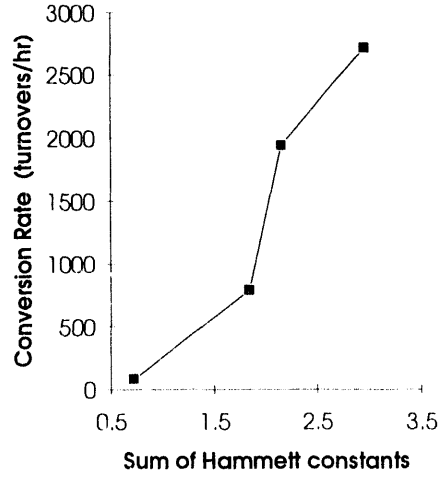

Figure 7. *Effect of electron withdrawing capacity of the substituents on catalytic rate (in turnovers/hr) of alcohol production (tertiary + secondary).*

We have previously found that Fe porphyrins with sums of substituent constants

above 1.00 give stable alkane-oxidation catalysts. Thus, all of the DPP series, except possibly FeDPP itself, should be stable and active. Indeed, all of the fluorinated FeDPP catalysts are completely stable in the reaction for at least a duration of one day, based on UV-visible absorption spectra of the catalyst obtained before and after a 24-hour run. In the future we will only use catalysts with strongly electron-withdrawing substituents in order to realize the full benefit in enhanced catalyst activity and stability.

The selectivity for hydroxylation at a particular carbon of isopentane is also influenced by the steric properties of the substrate binding cavity. For example, the percent yields of tertiary, secondary, and primary alcohol products of isopentane oxidation (83, 14, and 3%, respectively) for $FeDPPF_{20}$ are considerably altered when compared to selectivities for catalysts like $FeTPPF_{20}$, which does not have a substrate binding cavity (72, 26, and 2%). Further, $FeDPPF_{36}$ and $FeDPPF_{28}$ have nearly the same structure as $FeDPPF_{20}$, based on energy-optimization calculations, and would be expected to have similar selectivities. This is the case ($FeDPPF_{28}$: 82, 15, and 3%, $FeDPPF_{36}$: 85, 13, and 2%), and the selectivities for tertiary, secondary, and primary alcohols are also nearly constant with time for all three catalysts.

In comparison with selectivities previously measured for the first generation catalysts, the FeDPP series of catalysts give selectivities closest to those of FeOAATPP-OME (86, 13, and 1%), which likewise has bulky groups surrounding the cavity. For example, the FeDPPs give tertiary yields of 82-85% and secondary yields of 13-15%. In contrast, the catalysts with less bulky substituents forming the pocket ($FeOETPPF_{20}$) or with little (FeOMTPP) or no (FeTPP and $FeTPPF_{20}$) pocket give low relative tertiary alcohol yields (60-82%) and high secondary alcohol yields (17-35%).

We have initiated a resonance Raman study of the $FeDPPF_X$ series of catalysts to identify a spectroscopic marker of the electron-depletion effect of the substituents. The frequency of the ν_4 vibration of the porphyrin so far appears to follow the depletion order (FeDPP: 1344 cm^{-1}; $FeDPPF_{20}$: 1345 cm^{-1}; $FeDPPF_{28}$: 1347 cm^{-1}; $FeDPPF_{36}$: 1349 cm^{-1}). Redox potentials of the Fe(III)/Fe(II) couple are also a good indicator of the electron depletion of the macrocycle and may be more closely related to the catalytic activity of the iron center. Consequently, we are also measuring the redox potentials as shown in Figure 8. Note that a good correlation of the potential of the Fe(III)/Fe(II) couple with the Hammett constants is observed, validating our use of these parameters for predicting catalytic activity.

NMR Methane-Binding Studies. Studies of relative substrate binding energies have been completed using carbon-13 paramagnetic relaxation measurements with FeOMTPP and $FeOETPPF_{20}$ as the catalysts. Relaxation rates of ^{13}C-labeled substrate (halogenated methanes, benzene) were measured at different temperatures to determine enthalpies for binding of the substrate relative to dissolved $^{13}CO_2$. The measurements rely on the strong dependence on relaxation rates with distance from the paramagnetic Fe(III) at the center of the porphyrin. The relative enthalpies for binding to FeOMTPP are shown in Figure 9.

$FeOETPPF_{20}$ has a more well defined binding cavity for the halogenated methanes than does FeOMTPP. Clearly the halogenated methanes bind more strongly than benzene, the solvent

in our reactions. The binding energy for unsubstituted methane remains to be determined. The results in Figure 9 give little hope that methane will bind strongly under solvent conditions, but binding to the cavity may still be important in a gas phase environment.

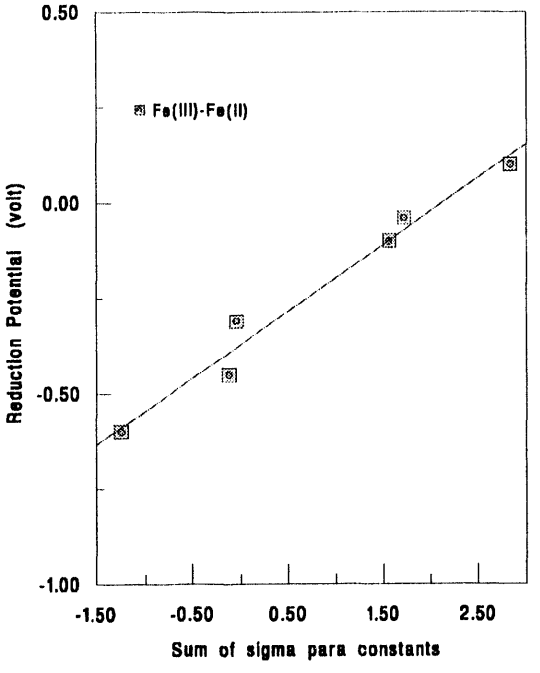

Figure 8. Dependence of Fe(III)/Fe(II) reduction potentials for iron porphyrins as a function of the electron-withdrawing capacity of the peripheral substituents. Least-squares fit for Fe(III)/Fe(II) couple is shown. Fe-porphyrins: FeOETPPCl, FeTPPCl, FeDPP, $FeDPPF_{20}Cl$, $FeDPPF_{28}Cl$ and $FeDPPF_{36}Cl$.

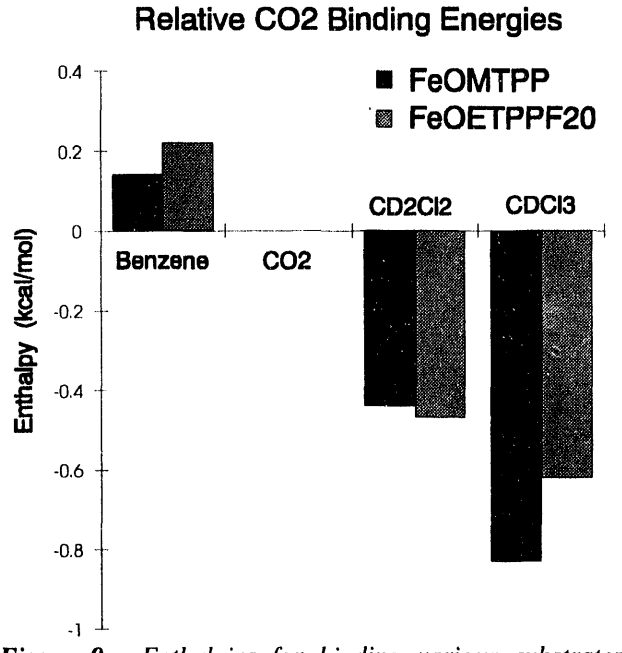

Figure 9. *Enthalpies for binding various substrates relative to CO_2 obtained from ^{13}C-NMR paramagnetic relaxation rates as a function of temperature. New data is for the cavity-bearing catalysts $FeOETPPF_{20}$ and is to be compared with the earlier data for FeOMTPP, which does not have a substrate cavity.*

Characterization of Advanced Catalyst Designs. Extensive structural characterization of the catalysts has been carried out and reported in detail in publications 10 through 17 listed below.

Summary. We have completed testing of a series of halogenated iron dodecaphenylporphyrin (FeDPP) catalysts by using both the iodosylbenzene shunt reaction and the molecular oxygen partial oxidation reaction at low temperatures (< 200° C). The series includes the fluorinated series $FeDPPF_X$, where x = 0, 20, 28, and 36. These catalysts show progressively higher catalytic activity as the degree of fluorination increases. Increasing activity was expected based on the increasing electron withdrawing capacity of the fluorinated substituents. In the $FeDPPF_X$ series, the electronic effect is almost surely the determinant of activity, because molecular modeling shows that the members of the series have almost identical conformations regardless of the number of fluorines. In the iodosylbenzene reaction, the $FeDPPF_X$ series shows novel selectivity properties, probably a result of the substrate binding cavity designed into its structure. The catalysts also have exceptional stability as a result of the electron withdrawing properties of the fluorinated phenyl substituents. In addition, a line in the resonance Raman spectrum has been identified as a marker of the electron withdrawing capacity of the substituents and thus the catalytic activity. We have also correlated activity with the potential of the Fe(III)/Fe(II) redox couple for the series. Both the reduction potential and the

Raman marker line frequency are good predictors of activity.

Plans:

In general, current plans call for developing a new, more active series of iron octaphenyl-tetranitroporphyrin (FeOPTNP) catalysts. This series offers the prospect of increased electron withdrawing capacity and substantially higher activity than the current FeDPP series. The parent catalysts, octaphenylporphyrin (OPP) and the meso-nitrated derivative, have been synthesized and Fe derivative are being prepared. Activity testing of the FeOPP and FeOPTNP series is the main goal for the next year. Studies in FY94 will focus on the O_2/air-oxidation reaction and, primarily, light hydrocarbons as a substrates. Efforts to design a supported catalyst for gas phase operation will also begin. All phases of the gas phase work will extend into FY95. Most of the motivation and justification for the proposed FY94 research goals is given in the preceding section. Specific research goals are listed below.

We also look forward to development of a formal relationship with W. R. Grace, Co. as an industrial partner in our work on partial oxidation of light hydrocarbons. After preliminary visits to Sandia by Rob Harding and James Idol this year, John Shelnutt will visit W. R. Grace on October 29, 1993, under a secrecy agreement, to discuss details of Grace's own work and current interests in the area. A CRADA is a likely outcome if matching funds can be found elsewhere.

Synthesis of Third Generation Catalysts. We will continue to try to synthesize $FeDPPF_{60}$ and also the chlorinated analogs of the fluorinated-FeDPP series (shown in Figure 13). We tried for about 9 months to synthesize the fully fluorinated Fe dodecaphenylporphyrin $FeDPPF_{60}$ but were unsuccessful with our current methods. We are now pursuing another method in collaboration with Prof. Richard LeGow at the University of Texas at Austin. This interesting new synthetic strategy leads, in general, to perfluorinated catalysts and involves direct fluorination of DPP. If this synthetic method works, any non-halogenated porphyrin could be perfluorinated to increase stability and activity.

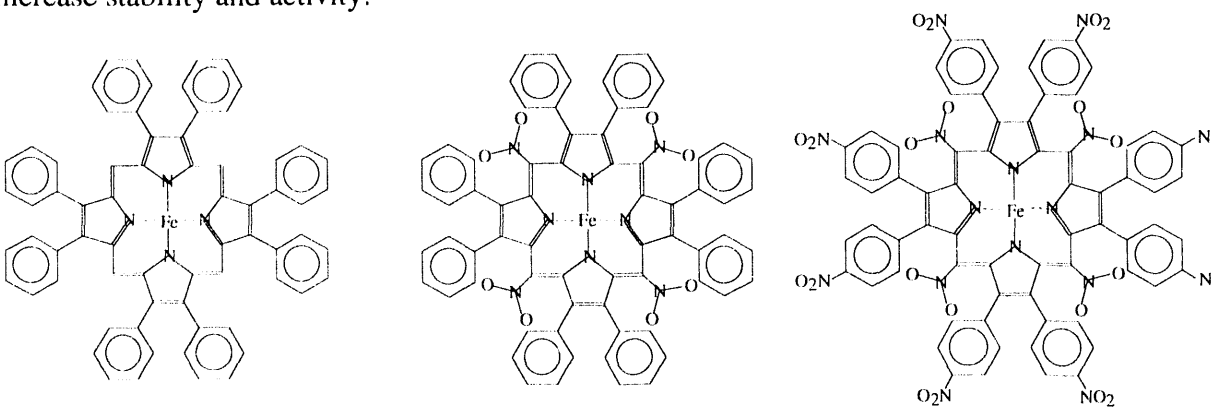

FeOPP $\Sigma\sigma_p = -0.08$ $\Sigma\sigma_m = 0.48$

$Fe(P)_8(NO_2)_4P$ $\Sigma\sigma_p = 3.04$ $\Sigma\sigma_m = 3.32$

$Fe(p\text{-}NO_2P)_8(NO_2)_4P$ $\Sigma\sigma_p = 4.96$ $\Sigma\sigma_m =$?

Figure 10. *New catalyst designs based on phenyl- and nitro-substituents. OPP and $(P)_8(NO_2)_4P$ have now been synthesized and the synthesis of the other catalysts are underway.*

We will synthesize FeOPP and its nitro analogs including those shown in Figures 10 and 11. These iron porphyrins are predicted to have enhanced catalytic activity and stability as described in the previous section. Also, Fe porphyrins like those in Figure 11 have improved solubility properties as described in the previous section.

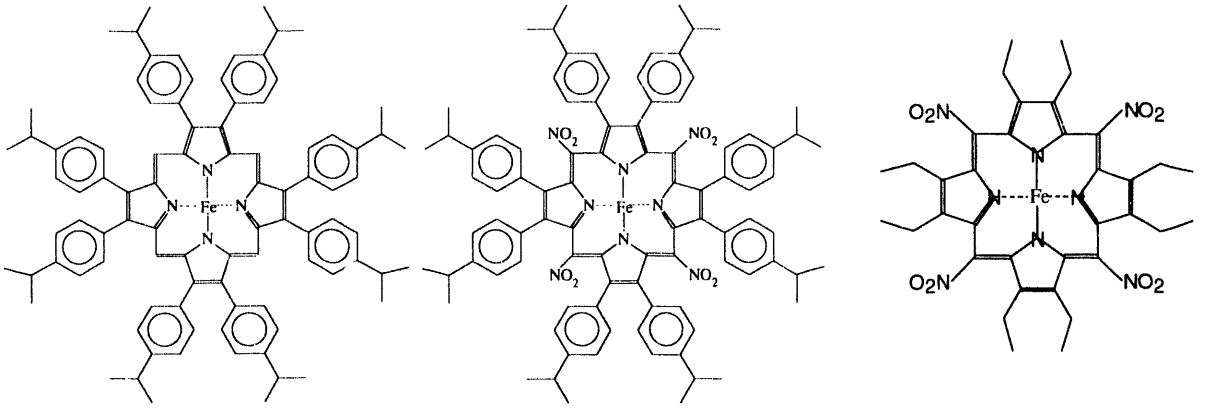

Fe(III) octa(p-isopropyl)-phenylporphyrin (FeO(isopropylP)P)
$\Sigma\sigma_p$ = -0.56

Fe(III) octa(p-isopropyl)phenyl-tetranitroporphyrin (FeO(isopropylP)TNP)
$\Sigma\sigma_p$ = 2.56

Fe(III) octaethyl-tetranitroporphyrin (FeOETNP)
$\Sigma\sigma_p$ = 1.92

Figure 11. *Other iron(III)-porphyrin catalysts to be synthesized and tested in FY94.*

Finally, we will synthesize Fe-derivatives of octa-acid-tetraphenylporphyrin-esters which have been modified with attached lipids for immobilization on supports, including the one shown in Figure 12. We will design other catalysts possessing carboxylic acid groups needed for immobilization and prepare the alumina-supported designed catalysts.

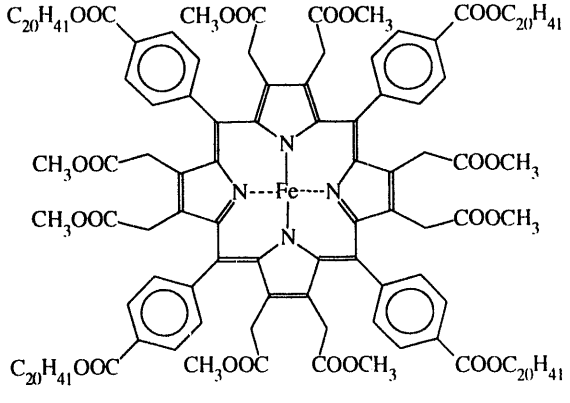

Figure 12. *Fe(III) octa-acetic acid-tetra(carboxyphenyl)porphyrin-octamethylester-tetra- iscosinate.* $\Sigma\sigma_p$ = *-0.04.*

Test Designed Catalysts. The synthesis effort is now generating many more catalysts than we can test with our single reactor. Also, we need more elaborate information about the reactions as a function of temperature, pressure, and time. This new information would help to determine reaction mechanisms which will in turn guide further molecular design work toward

improving activity and stability of the catalysts. Consequently, in order to enhance the testing program for the O_2/air-oxidation reaction, we have ordered two more of the teflon-lined reactors from Berghoff/America ($30K). Currently, one test run takes about a day to run; with the additional reactors we will be able to carry out three tests per day instead of the one. Also, the new reactors are equipped with gas and liquid GC sampling capabilities which will allow us to follow the reaction in time.

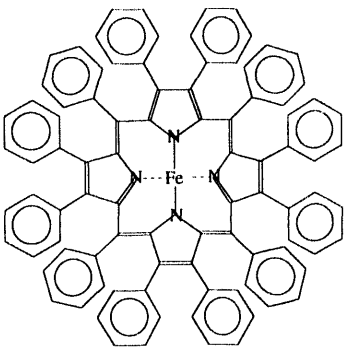

Fe(III)Dodecaphenylporphyrin (FeDPP)
$\Sigma\sigma_p$ = -0.12 **$\Sigma\sigma_m$ = 0.72**

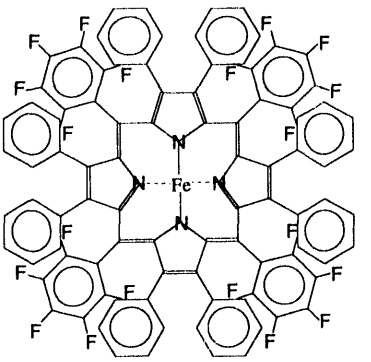

Fe(III)DodecaphenylporphyrinF$_{20}$ (FeDPP-F$_{20}$)
$\Sigma\sigma_p$ = 1.56 **$\Sigma\sigma_m$ = 1.84**

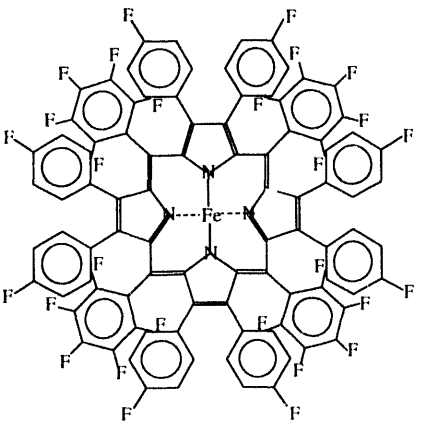

Fe(III)DodecaphenylporphyrinF$_{28}$ (FeDPP-F$_{28}$)
$\Sigma\sigma_p$ = 2.36 *(est. 0.09)* **$\Sigma\sigma_m$ = 2.16** *(est. 0.10)*

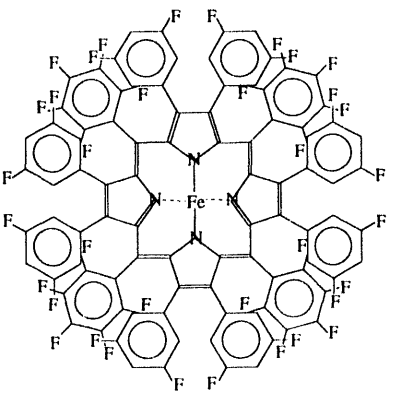

Fe(III)DodecaphenylporphyrinF$_{36}$ (FeDPP-F$_{36}$)
$\Sigma\sigma_p$ = 2.84 *(est. 0.15)* **$\Sigma\sigma_m$ = 2.96** *(est. 0.20)*

Figure 13. *Structures of the Fe(III) derivatives of fluorinated dodecaphenylporphyrins. All of these porphyrins have now been synthesized. The sum of the Hammett substituent constants (para and meta) give a measure of electron withdrawing capability of the substituents.*

We will first complete the testing of the Fe and Mn derivatives of the fluorinated dodecaphenylporphyrin catalysts shown in Figure 13 using the air-oxidation reaction with isopentane, methane and ethane for the most active members of the group. We will also optimize the conditions for air oxidation of isopentane, methane, and ethane. We will test other halogenated DPPs that we successfully synthesize.

We will test the derivatives of FeOPP, including the nitro-derivatives of this catalyst shown in Figures 10 and 11, assuming we are successful in synthesizing these in FY94. We expect that the synthesis of at least a few of these catalysts will be possible based on initial results

described in the previous section. We will test all of these new catalysts in iodosylbenzene reaction as well as the O_2-oxidation reaction with methane, ethane, and isopentane substrate. We will also test the supported Fe-porphyrin catalysts, including the lipo-porphyrin shown in Figure 12.

NMR Substrate Binding Studies. We will carry out alkane binding with at least one member of the fluorinated FeDPPs, probably the F_{20} derivative. Should molecular modeling indicate a candidate porphyrin with a substantially improved methane binding affinity, we will also perform NMR binding studies for this designed catalyst with methane.

Characterization of Advanced Catalyst Designs. All catalysts available to us by the end of 1993 will be fully characterized by NMR, UV-visible absorption spectroscopy, resonance Raman spectroscopy and other techniques.

FY95 Goals. Tasks include: (1) continued light-hydrocarbon-oxidation testing of catalysts synthesized in 1994, (2) demonstration of gas-phase methane oxidation and binding of methane to the advanced catalyst designs, (3) optimization of light hydrocarbon oxidation under gas phase conditions, (4) structural characterization of catalysts synthesized in 1994, and (5) studies of large scale batch and flow-thru reactor designs.

Publications:

1. "Excited State Transient of Vanadyl Uroporphyrin I Detected Using Resonance Raman Spectroscopy" Alden, R. G.; Sparks, L. D.; Ondrias, M. R.; Crawford, B. A.; Shelnutt, J. A., J. Phys. Chem. **1990**, 94, 1440.
2. "Transient Raman Difference Spectroscopy of Nickel(II)-Uroporphyrin π–π Complexes" Crawford, B. A.; Ondrias, M. R.; Shelnutt, J. A., J. Phys. Chem. **1990**, 94, 6647.
3. "Photochemically-Driven Biomimetic Oxidation of Alkanes and Olefins" Shelnutt, J. A.; Trudell, D. E., in "Novel Materials in Heterogeneous Catalysis" Eds. Baker, R. T. K.; Murrell, L. L., ACS Symposium Series 437, (American Chemical Society: Washington) Chpt. 24, 1990.
4. "Tetracycloalkenyl-meso-Tetraphenylporphyrins as Models for the Effect of Non-Planarity on the Light Absorption Properties of Photosynthetic Chromophores" Medforth, C. J.; Berber, M. D.; Smith, K. M.; Shelnutt, J. A., J. Am. Chem. Soc. **1990**, 31, 3719.
5. "Nonplanar Distortion Modes for Highly Substituted Porphyrins" Medforth, C. J.; Senge, M. O.; Smith, K. M.; Sparks, L. D.; Shelnutt, J. A., *J. Am. Chem. Soc.* **1992**, 114, 9859-9869. SAND91-2458J.
7. "Relationships between Structural Parameters and Raman Frequencies for Some Planar and Non-Planar Nickel(II) Porphyrins" Shelnutt, J. A.; Medforth, C. J.; Berber, M. D.; Barkigia, K. M.; Smith, K. M., J. Am. Chem. Soc. **1991**, 131, 4077-4087.
8. "The Effects of π–π Interactions on the Molecular Structure and Resonance Raman Spectra of Crystalline Copper(II) Octaethylporphyrin" Sparks, L. D.; Scheidt, W. R.; Shelnutt, J. A., *Inorg. Chem.* **1992**, 31, 2191-2196. SAND91-1794J.
9. "Metal-Dependence of the Nonplanar Distortion of Octaalkyl-Tetraphenylporphyrins" Sparks, L. D.; Medforth, C. J.; Park, M.-S.; Chamberlain, J. R.; Ondrias, M. R.; Senge,

M. O.; Smith, K. M.; Shelnutt, J. A., *J. Am. Chem. Soc.* **1992**, 115, 581-592. SAND91-2007J.

10. "Raman Spectroscopic Characterization of Isomers of Copper and Zinc N-Phenyl-protoporphyrin IX Dimethyl Ester" Sparks, L. D.; Chamberlain, J. R.; Hsu, P.; Swanson, B. A.; Ortiz de Montellano, P. R.; Shelnutt, J. A., *Inorg. Chem.* **1993**, 32, xxxx-xxxx.
11. "Molecular Design of Substrate Binding Sites" Shelnutt, J. A.; Hobbs, J. D., *ACS Fuel Div. Preprints*, **1992**, 37, 332-339. SAND91-2921C.
12. "Resonance Raman Spectroscopy of Non-Planar Nickel Porphyrins" Shelnutt, J. A.; Majumder, S. A.; Sparks, L. D.; Hobbs, J. D.; Medforth, C. J.; Senge, M. O.; Smith, K. M.; Miura, M.; Luo, L.; Quirke, J. M. E., *J. Raman Spectrosc.* **1992**, 23, 523-529. SAND92-0743J.
13. "Computer Modeling Opportunities in Catalysis Research" Carlson, G. A.; Shelnutt, J. A., Massively Parallel Computing Res. Lab. Research Bulletin. SAND91-2121J.
14. "Synthesis and Spectroscopic Studies of Octa-acetic acid-tetraphenylporphyrins" Miura, M.; Renner, M. W.; Majumder, S. A.; Martinez, S. L.; Hobbs, J. D.; Shelnutt, J. A. *Angew. Chemie* 1993, submitted.
15. "Macrocycle and Substituent Vibrational Modes of Nonplanar Nickel(II) Octaethyl-tetraphenylporphyrin from Its Resonance Raman, Near-Infrared-Excited FT Raman, and FT-IR Spectra and Deuterium Isotope Shifts" Stichternath, A.; Schweitzer-Stenner, R.; Dreybrodt, W.; Mak, R. S. W.; Li, X.-Y.; Sparks, L. D.; Shelnutt, J. A.; Medforth, C. J.; Smith, K. M. *J. Phys. Chem.* **1993**, 97, 3701-3708.
16. "A Planar Dodecasubstituted Porphyrin" Senge, M. O.; Medforth, C. J.; Sparks, L. D.; Shelnutt, J. A.; Smith, K. M. *Inorg. Chem.* **1993**, 32, 1716-1723.
17. "The Planar-Nonplanar Conformational Equilibrium in Metal Derivatives of Octaethylporphyrin and Meso-Nitro-Octaethylporphyrin" Anderson, K. K.; Hobbs, J. D.; Luo, L.; Stanley, K. D.; Quirke, J. M. E.; Shelnutt, J. A. *J. Am. Chem. Soc.* **1993**, in press.

Relevant Patents: 1990-Present

(1) "Process for Light-Driven Hydrocarbon Oxidation at Ambient Temperatures" J. A. Shelnutt, U.S. Patent No. 4,917,784 (Apr. 17, 1990).
(2) "Improved Catalysts for Air Oxidation of Light Alkanes to Oxygenates" J. A. Shelnutt, Patent Disclosure SD-4947, S-73,031 (Jan. 14, 1991).
(3) "Sterically Hindered Porphyrins for Fuel Catalysts" M. Miura, J. A. Shelnutt, Patent Disclosure, in preparation, (Sept. 15, 1993).
(4) "Photocatalytic Conversion of Substances Using Organometallic Dyes and Light" S. A. Majumder, J. A. Shelnutt, M. R. Prairie, M. R. Ondrias (SD-5112, S-75,556), Ser. No 08/042,275 (Apr. 1, 1993).

FULLERENE-BASED CATALYSTS FOR METHANE ACTIVATION

A. S. Hirschon, R. Malhotra, R. B. Wilson and H-J Wu
SRI International, Menlo Park, CA 94025

ABSTRACT

The purpose of this project is to investigate fullerene based catalysts for the conversion of methane into higher hydrocarbons. In this beginning phase of the project we have developed methods to produce fullerene soot and metallized fullerene soot and are now in the process of examining the reactivities of fullerene soot with hydrogen and methane. We have found that the soot is an excellent catalyst for shuttling hydrogen and may aid in hydrogenation reactions. When soot is treated with methane at high temperatures it appears to activate the C-H bond allowing methane conversions at temperatures lower than found necessary under purely thermal conditions. Furthermore, under these conditions, soot catalysis forms essentially only ethane and ethylene in the product stream, with minimal amounts of aromatics or acetylenes. We are now in the process of determining the effect of reaction conditions such as added hydrogen on the extent of coking and product distribution.

PROJECT OBJECTIVES

The objectives of this project are to develop techniques for production of fullerene-based catalysts and examine the reactivities of these catalysts for conversion of methane into higher hydrocarbons. We plan to prepare both pure carbon fullerene catalysts and metallized fullerene based catalysts and study their abilities to promote carbon-hydrogen bond activation, with the goals of selectively producing ethane and ethylene from methane.

INTRODUCTION

Methane is one of the most abundant sources of energy and is found naturally in underground reservoirs and as a by-product of indirect coal liquefaction processes. Although methane is useful as a fuel, it is not easily stored or transported, and for that reason, the efficient direct conversion of methane to higher hydrocarbons is essential to provide an economical alternative energy source. The main difficulty in converting methane is the production of undesirable side products. Oxidation methods easily convert

methane to higher hydrocarbons, but overoxidation to CO_2 makes it an uneconomical method. Alternatively, simple thermal decomposition of methane also makes higher hydrocarbons; however, the production of liquid fuels from methane by this method is not yet economically feasible because of the high C-H bond strength of methane compared with that of possible products. At the high temperatures required to activate methane, the C_2 products formed will further decompose and produce still higher hydrocarbons, aromatics, and coke.

To overcome these problems and make these pyrolysis reactions more economically feasible for direct conversion of methane into higher hydrocarbons, we are now evaluating the recently discovered fullerenes.[1] Fullerenes are a new allotrope of carbon consisting of closed-shell cages of sixty or more carbon atoms. The most celebrated of these caged molecules, C_{60}, has a highly symmetric soccer-ball structure in which all sixty carbon atoms are equivalent (Figure 1). C_{60} has been named buckminsterfullerene in honor of the architect, Buckminster Fuller, who developed the geodesic structures consisting of pentagons and hexagons. Unlike other forms of carbon, fullerenes are soluble in solvents like benzene and toluene and are vaporizable at modest temperatures because of their "molecular" nature. The vapor pressure of C_{60} itself is about 1 Torr at 800°C. We believe that the insoluble portion of the soot consists of either larger fullerenes or crosslinked smaller, imperfect, fullerenes. In any event, the soot itself may also present a unique fullerene-like surface and hence is worth testing. All carbon atoms in fullerenes are sp^2 and form a three-dimensional fully conjugated aromatic system.

Fullerenes possess unique properties, including the ability to shuttle H atoms, act as electrophiles and to stabilize methyl radicals and readily accommodate organic radicals. This ability to act as "radical sponges" is presumably because the radical adducts are

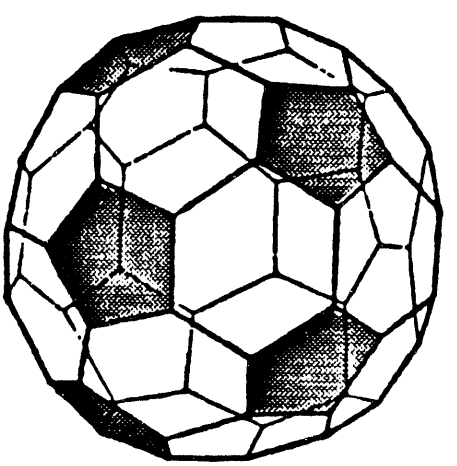

Figure 1. Structure of C_{60}, Buckminsterfullerene.

stabilized by the conjugated π-system. We suggest that catalysts based on C_{60} and other fullerenes will provide a facile pathway to convert methane into higher hydrocarbons, and since these catalysts are easily produced in soot, they can potentially be inexpensive catalysts and make the direct conversion of methane into higher hydrocarbons inexpensive and environmentally sound.

Direct coupling of methane can be achieved thermally without catalyst. Some of the important parameters to be considered are cracking temperature, residence time, and diluent gas. However, for direct coupling to be economically competitive, selectivity needs to be increased and coking decreased, and temperatures need to be reduced as low as possible. The key to these pyrolysis reactions is to generate methyl radicals, which then polymerize into higher hydrocarbons. However, current methods are thought to produce the radicals in the gas phase, which may lead to indiscriminate reactions and coke formation. In contrast, fullerenes, which have a great affinity for radicals, are expected to add methyl radicals and thereby provide for more selective reactions. Another attribute of these fullerenes is that they can easily incorporate metals either inside or outside the cage structure.[1-3] Some of these metals may impart to the fullerenes properties that will aid in producing methyl radicals.

A second reason why fullerenes may be effective catalysts for methane activation is their strong electrophilic character. Recent work shown by Sen et al.[4] has shown that methane may be activated by electrophilic agents. C_{60} and C_{70} fullerenes display remarkable electrophilic characteristics including direct amination with primary and secondary amines and a very low first reduction potential of -0.5 V (vs. NHE). Wudl[5] has characterized fullerenes as, "electrophiles par excellence."

APPROACH

The focus of the proposed work is to prepare and examine fullerene-based catalysts for converting methane into higher hydrocarbons. There are several methods of producing fullerene soot such as by laser pyrolysis and electrode discharge on carbon electrodes. We are attempting to develop large scale efficient methods to produce fullerene soot. The commonly used arc method for making fullerenes produces large amounts of soot, which contains up to 20% of extractable (and vaporizable) fullerenes such as C_{60} and C_{70}. We believe that the insoluble portion of the soot consists of either larger fullerenes or cross-linked smaller, imperfect, fullerenes. In any event, the soot itself may also present a unique fullerene-like surface and hence is worth testing. Besides testing the fullerenes and soots by themselves, we will also prepare many catalysts in which metals known to activate methane will be attached to the fullerenes. The idea is that the methyl radicals, produced at

the active metal site, will spill over to the fullerene surface where they will reside long enough to encounter other methane (or methyls) and be converted to higher hydrocarbons.

One of the novelties of these fullerene preparations is that other atoms can be incorporated into the structure: inside the cage, outside the cage, or within the framework itself. For example, Smalley et al. produced a series of fullerenes containing lanthanum incorporated inside the cage by using graphite which had been impregnated with La.[2,3] Other workers such as Roth et al. have synthesized ferrocene complexes with the metal speculated to be in a clamshell configuration.[6] Furthermore, Smalley et al. also produced fullerenes with boron incorporated in the framework.[7] All these variations may impart unique chemical properties to the fullerenes, and these will be explored in later phases of this work.

ACCOMPLISHMENTS AND CONCLUSIONS

Preparation of Soot

We have developed a large scale preparative reactor based on the arc-discharge method of Hauffer et al.[8] which incorporates a computer controlled graphite electrode feeder and a load/lock port to facilitate changing the graphite rods without having to break vacuum. Using these methods we can prepare carbon soot which contains 12-14% of fullerenes. The fullerenes can easily be extracted from the carbon soot by toluene to yield mainly C_{60} and smaller amounts of C_{70} and higher fullerenes. However, for the initial phase of the methane activation studies, we will use the fullerene containing soot.

To prepare metallized soot (and fullerenes) we drill the graphite anode and pack it with the metal of interest, or, in case the metal is very volatile, with a suitably refractory compound like the carbide or oxide, into the reactor electrodes holes. Using this set-up, we prepared small amounts of metallized soot from the first row transition metals, including Ni, Fe, Cu, Cr, V and Mn. For these runs, we used 12-in long 5/16-in dia graphite rods as anodes. The rods were drilled 5 to 6 in deep with a 1/8- or 3/16-in id hole. After packing the rods, the ends were capped with a ca. 3/8-in long plug of graphite. The stationary cathode was a 1/2-in dia. graphite rod. During the run the gap between the electrodes was maintained between 5 and 8 mm; the current varied between 125 and 150 amps, and the potential difference was ca. 30 V. The yield of extractable fullerenes under these conditions is generally low (ca. 1-2%) mainly because of the presence of oxygen.

The metal content was determined by oxidizing the soot using a TGA and recording the remaining ash (metal oxide). The soot was oxidized in synthetic air using a temperature ramp of 10°C/min from room temperature to 1000°C with a hold time of 60 minutes at

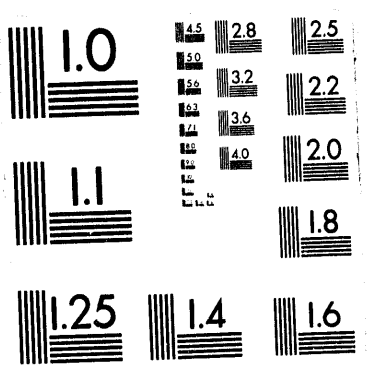
1.0
1.1
1.25
1.4
1.6
1.8
2.0
2.2
2.5
2.8
3.2
3.6
4.0
4.5
5.0
5.6
6.3
7.1
8.0
9.0

4 of 8

750°C to ensure a controlled and complete oxidation. Table I lists the ash contents for these soots as determined by this method. Assuming the state of the metal as listed in this table, the final Wt% of the metal was determined to range from 10.6% for V to 18.1% for Ni, or At% of 2.8 to 4.5%, respectively.

Selected soots were analyzed by X-ray diffraction techniques and TEM for estimates of particle sizes and morphology. The Fe-soot sample was analyzed by TEM and the Fe was found to be evenly distributed in 3 to 10 nm particles throughout the soot.

Table 1

TGA ANALYSIS AND METAL CONTENT OF THE VARIOUS METALLIZED SOOTS

Metal	At.Wt	Oxide (valency)	Mol Wt	Residue, Wt%	Wt %	At %
V	50.9	5	181.8	18.9	10.6	2.7
Cr	52.0	3	152.0	20.3	13.9	3.6
Fe	55.9	3	159.7	17.1	12.0	2.8
Ni	58.7	4	90.7	27.9	18.1	4.3
Cu	63.5	2	79.5	20.3	16.2	3.5

Hydrogen-Transfer Reactions Catalyzed by Fullerenes

As mentioned above, a strong rationale for using fullerene-based catalysts for methane activation is their ability to shuttle hydrogen. It is therefore appropriate to summarize the results (obtained under a separate research program) as background.

Previous work at SRI on coal liquefaction under PETC sponsorship had focused attention on the importance of H-transfer induced cleavage of strong bonds.[9] This work led to the recognition of the importance of H-acceptors along with H-donors and provided a chemical basis for rationalizing improved conversions often observed when part of the donor component is replaced by a purely aromatic species, H-acceptors.[10]

Fullerenes are like polycyclic aromatic hydrocarbons, except that they do not have any hydrogens. Hence, we tested the ability of C_{60} and C_{70} to facilitate the cleavage of 1,2'-dinaphthylmethane in several aromatic-hydroaromatic mixtures at 400°C. We have previously used this system extensively in our model compound studies. In all cases, fullerenes enhanced the rate of cleavage as well as increased the selectivity of H-transfer to the 1-position giving 2-methylnaphthalene.[10,11] The increased reactivity reactivity, in concert with increased reactivity, means that not only did the fullerenes convert the existing H-transfer species to more stable (and hence more selective) ones, but also increased the pool of H-transfer species to more than compensate for the reduced reactivity.

Furthermore, we noticed that the hydroaromatic component was almost completely dehydrogenated in the fullerenes and only partly so in their absence.[11] Analysis of the fullerenes in the reaction mixture after short periods (one to two hours) showed conversion of C_{60} to hydrogenated species, $C_{60}H_x$ (x = 2 to 36), which upon prolonged heating (7 h), reverted to C_{60}. These experiments demonstrate the ability of C_{60} to undergo facile transfer hydrogenations.

In separate experiments we showed that C_{60} can also be hydrogenated with molecular H_2 in a purely thermal system (no added catalyst). Heating C_{60} with H_2 (1000 psi cold) to 400°C for 2 h produced variously hydrogenated C_{60} species. Thus, C_{60} was able to "activate" the 104-kcal/mol H–H bond. In view of these results, it seems reasonable that C_{60}, and other fullerenes, can also activate the 105-kcal/mol bond in methane.

Methane Activation Experiments

In order to test these fullerene soots we have constructed a dual furnace reactor system where the methane is first heated in a preheating furnace and then passed into a high temperature furnace with a short heating zone (4") which leads to a cool quenching zone to minimize any possible thermal reactions after conversion. We have just started to examine the fullerene soot for methane activation and are now developing the base-line conditions for testing of these materials. We have found that under our testing conditions the soot can catalyze the reaction at approximately 100-150°C lower temperatures than for the thermal reactions and produces mainly ethane and ethylene as the gaseous products. Figure 2 shows the typical light gas product distribution as a function of flow rate for the soot catalyzed methane decomposition (2a) compared to a thermal decomposition (2b) using pure methane gas (with 7% argon as internal standard). Under these conditions the thermal reactions gave tar and coke whereas the soot catalyzed reactions also gave coke, but no tar. We are now studying these soot catalyzed reactions in the presence of hydrogen.

We also analyzed fullerene soot which was used for activating methane, using SRI's home-built surface analysis by laser ionization instrument (SALI). This instrument was able to detect variations in the soot after exposure to methane and ethylene at 900°C. For instance, as shown in Figure 3, small amounts of masses with additions of CH_3 groups on the C_{60} were detected, and in comparing spectra of the C_{60} (Figure 4a) to that of C_{60} exposed to methane (Figure 4b) we see evidence of hydrogenated C_{60}. Furthermore when the soot was treated with ethylene, masses consistent with hydroaromatics were also detected (Figure 5), but it is not clear if these masses were catalyzed by the fullerenes, or they were formed from the normal decomposition of ethylene. In future work we hope to be able to correlate the fate of the methane on the soot after long term reactions.

PLANS

During the coming year we plan on testing the fullerene soot and fullerene depleted soot for methane conversion and determine the effect of added H_2 and other gases on the product distribution and coking propensity. Metallized soots will also be examined to determine their respective effects on threshold temperatures, product distribution, and coke formation.

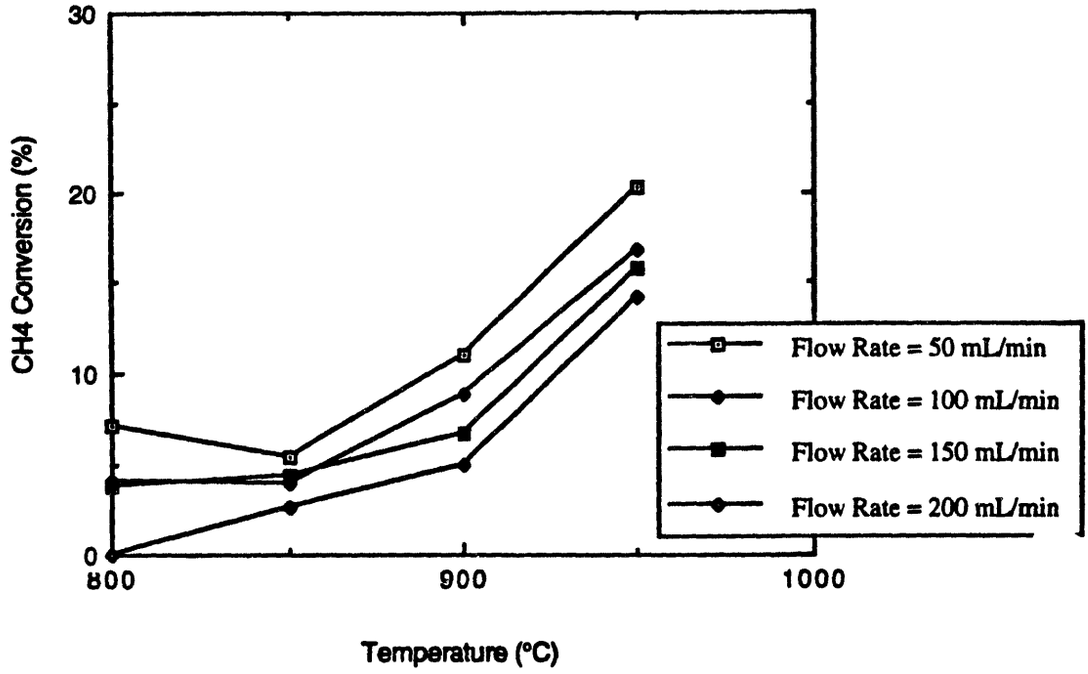

Figure 2a. Soot catalyzed methane activation.

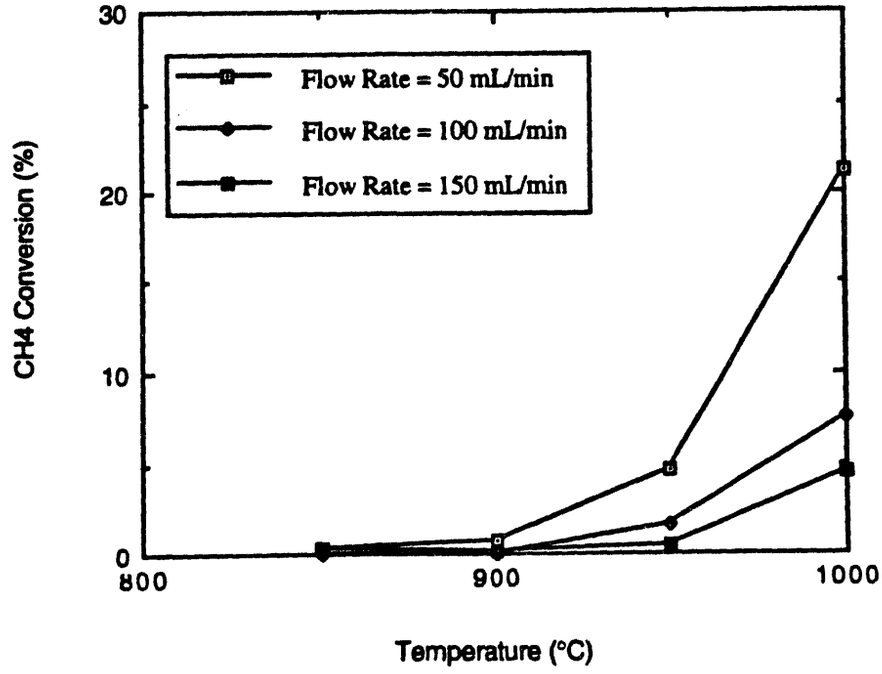

Figure 2b. Thermal methane activation.

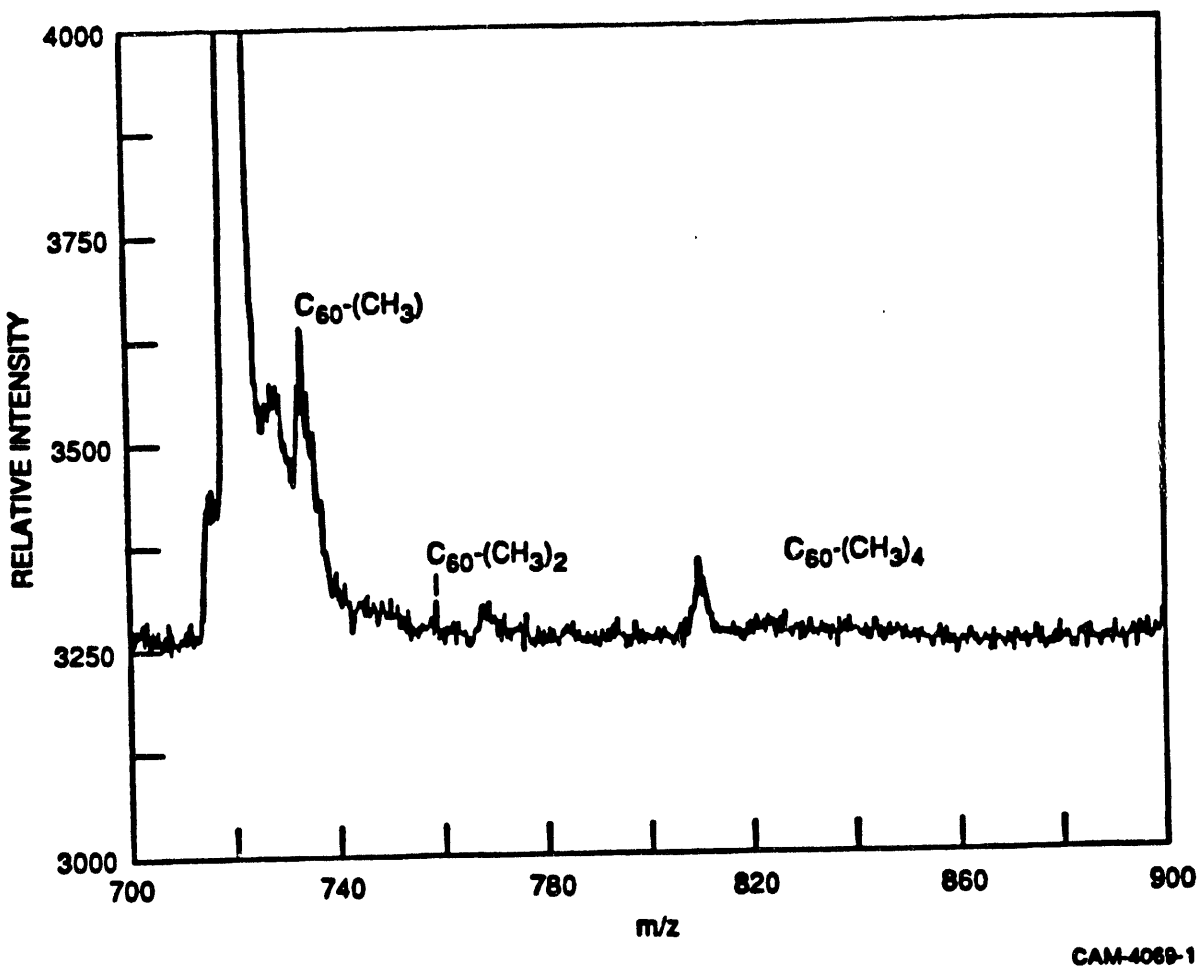

Figure 3. SALI spectrum of soot treated with methane at 900°C.

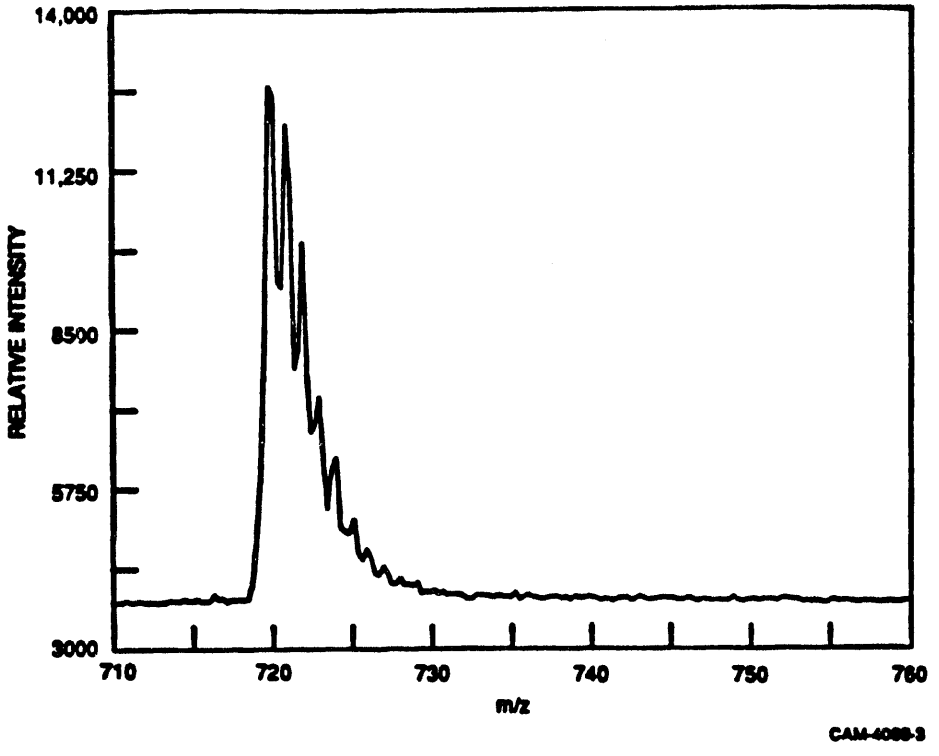

Figure 4a. SALI spectrum of soot treated with methane at 900°C.

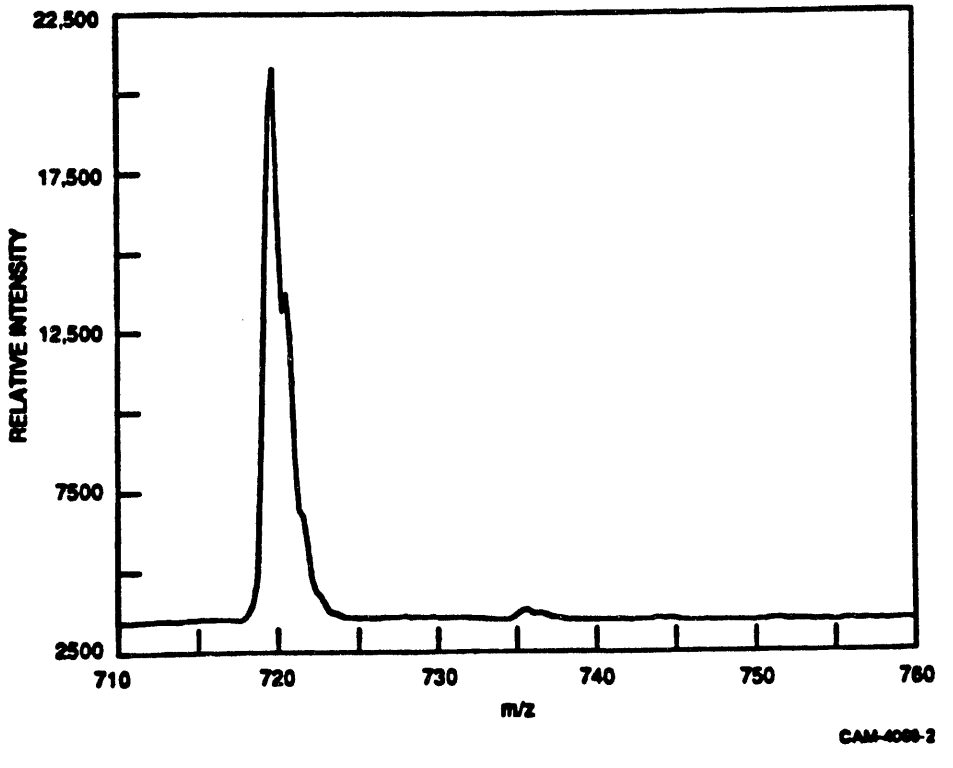

Figure 4b. SALI spectrum of soot.

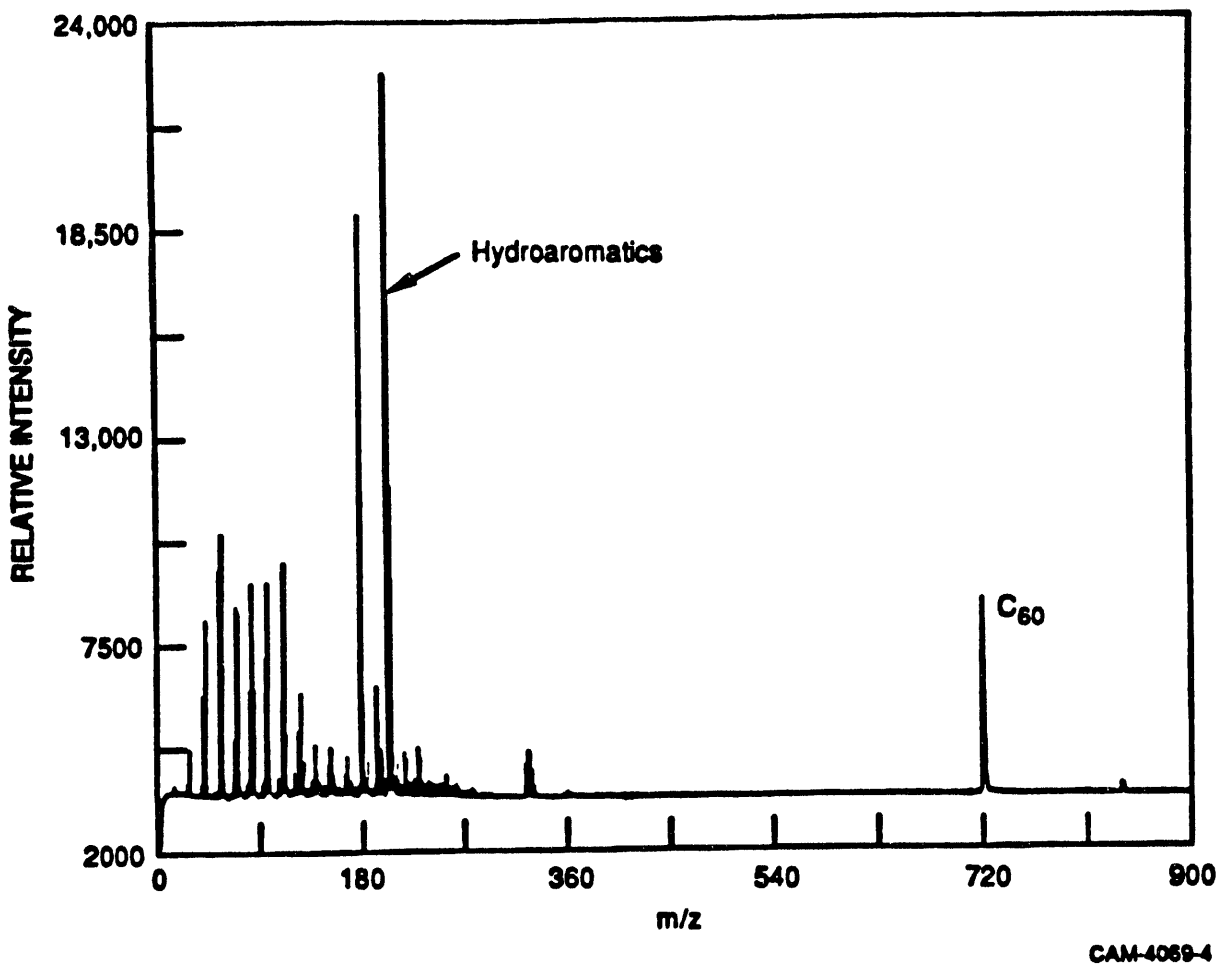

Figure 5. SALI spectrum of soot treated with ethylene at 900°C.

REFERENCES

1. Accounts of Chemical Research 1992, **25**, pp 97-169, entire issue devoted to fullerenes.

2. R. Baum, R. Dagani, Chemical and Engineering News 1991, **69**, 6-7.

3. F. D. Weis, J. L. Elkind, S. C. O'Brian, R. F. Aul, and R. E. Smalley. J. Am. Chem.Soc. 1988, **110**, 4464-4465.

4. E. Gretz, T. Oliver, and A. Sen, J. Am. Chem. Soc. 1987, **109**, 8109-8111.

5. Wudl, F.; Hirsch, A.; Khemani, K. C.; Suzuki, T.; "Survey of Chemical Reactivity of C60, Electrophile and Dieno-polarophile Par Excellence." in Fullerenes, Hammond, G. S., and Kuck, V. J. Editors, ACS Symposium Series 481; Atlanta, 1991, Am. Chem. Soc., Washington, D.C., 1992, p. 161.

6. L. M. Roth, Y. Huang, J. T. Schedler, C. J. Cassady, Q. Ben-Amotz, B. Kahr, and B. S. Freiser, J. Am. Chem. Soc., 1991, **113**, 6298-6299.

7. T. Guo, C. Jin, and R. E. Smalley, J. Phys. Chem. 1991, **95**, 4948-4950.

8. Haufler, R. et al., J. Phys. Chem. 1990, **94**, 8634.

9. McMillen, D. F.; Malhotra, R.; Hum, G. P.; Chang, S.-J. *Energy Fuels* **1987**, *1*, 193.

10. Malhotra, R.; McMillen, D. F. *Energy Fuels* **1993**, *7*, 227.

11. Malhotra, R., McMillen, D. F.; Tse, D. S.; Lorents, D. C.; Ruoff, R. S.; Keegan, D. M.*Energy Fuels* **1993**, *7*, xxxx.

DEVELOPMENT OF VANADIUM-PHOSPHATE CATALYSTS FOR METHANE PARTIAL OXIDATION

Robert L. McCormick
Mahesh C. Jha
Robert D. Streuber
Amax Research & Development Center
5950 McIntyre Street
Golden, Colorado 80403

Presented at
U. S. Department of Energy
Pittsburgh Energy Technology Center
Coal Liquefaction and Gas Conversion
Contractors' Review Conference
Pittsburgh, Pennsylvania
September 27 - 29, 1993

Contract No. DE-AC22-92PC92110
October 1, 1992 - March 31, 1995

PROGRAM OBJECTIVES

The United States has vast natural gas reserves which could contribute significantly to our energy security if economical technologies for conversion to liquid fuels and chemicals were developed. Many of these reserves are small scale or in remote locations and of little value unless they can be transported to consumers. For natural gas, transportation is economically performed via pipeline, but this route is usually unavailable in remote locations. Another option is to convert the methane in the gas to liquid hydrocarbons such as methanol which can easily and economically be transported by truck. Therefore, the conversion of methane to liquid hydrocarbons has the potential to decrease our dependence upon oil imports by opening new markets for natural gas and increasing its use in the transportation and chemical sectors of the economy.

Furthermore, indirect coal liquefaction processes produce a significant quantity of methane. Conversion of this methane to a liquid fuel could enhance the economics of indirect liquefaction.

The goal of this project is to develop a catalyst which allows methane oxidation to methanol to be conducted at high conversion and selectivity. To achieve a high conversion, we require a catalyst which is active at less than 500°C so that higher feed gas oxygen content can be employed. Ideally, air will be used as the source of oxygen. Achievement of high selectivity will require a highly selective catalyst and optimization of process conditions. Vanadium phosphate (VPO) catalysts were selected for study because they have demonstrated the capability to selectively oxidize other alkanes at relatively low temperature and are used commercially. VPO catalysts prepared and activated by various methods are being tested in a process variable study. Further catalyst development will involve the use of promoters and supports to improve activity and selectivity.

The project is divided into four tasks:

- Task 1. Laboratory Setup

  Equipment for catalyst preparation and reactivity testing was set up and tested. Gas analytical procedures were developed. Blank reactor runs were conducted. The duration of this task was October 1, 1992 through December 31, 1992.

- Task 2. Process and Catalyst Variable Study

  Tests are being conducted to determine the effect of temperature, pressure, CH_4/O_2 ratio, H_2O/CH_4 ratio, space velocity, and catalyst P:V ratio on activity and selectivity in methane partial oxidation. This task will be completed by October 31, 1993.

- Task 3. The Effect of Promoters and Supports

  Under this task, we will attempt to improve the activity and selectivity of the catalyst through the use of promoters and supports. Several promoters and supports will be tested. Catalyst characterization by XRD and FTIR will provide a fundamental understanding of these effects. The duration of this task is October 1, 1993 through July 31, 1994.

- Task 4. Advanced Catalyst Testing

  Advanced catalysts which are both promoted and supported will be prepared. These catalysts will be tested in runs of relatively long duration (200 hours) to determine long-term activity, selectivity, and stability in methane oxidation to methanol. The duration of this task is August 1, 1994 through March 31, 1995.

ACCOMPLISHMENTS

During the first year of this program, effort was focused on three areas:

- Synthesis of the vanadium phosphate catalyst precursor.
- Activation of the precursor to produce vanadyl pyrophosphate, the active and selective phase in hydrocarbon oxidation catalysis.
- Testing of the catalyst in a process variable scoping study.

Synthesis of the catalyst precursor has been accomplished using both organic and aqueous reaction media. The identity of the precursor phase was confirmed by X-ray powder diffraction (XRD). Catalyst activation to form $(VO)_2P_2O_7$ was found to be very sensitive of activation conditions, in agreement with published work (Hodnett, 1985). Activation by heating to 400°C in air, followed by heating to 500°C in nitrogen or a reducing atmosphere, yielded the desired phase. Performing the 500°C step in nitrogen containing a few percent steam led to a highly crystalline material thought to be similar to equilibrium catalysts used industrially for butane oxidation (Cornaglia et al., 1991). However, activation with steam led to a reduction of the P:V molar ratio to a level below one. This may be detrimental to catalyst selectivity (Horowitz et al., 1988).

Catalyst testing is ongoing. Results available to date indicate that under high CH_4/O_2 conditions, a VPO catalyst prepared in organic media (VPO_{org}) and activated in steam/nitrogen is highly active for methane conversion to carbon monoxide. Significant methane conversion was observed over this catalyst at 1 atm and 450°C. This compares to a temperature of 500°C for a V_2O_5/SiO_2 catalyst. No methanol or formaldehyde has been observed for the VPO_{org} catalyst under the test conditions utilized so far. Selectivity to CO was above 90 percent for this catalyst. A VPO

catalyst prepared in aqueous HCl (VPO_{aq}) and activated in steam was less active, exhibiting conversion at 500°C. Carbon monoxide selectivities were near 60 percent, with the balance being CO_2. These results show that the VPO_{org} catalyst is highly active for methane conversion. Because the predominant product is CO rather than CO_2, there is some hope that altering reaction conditions or modifying the catalyst will lead to the formation of methanol or formaldehyde. Future testing will investigate the effect of the CH_4/O_2 ratio, adding steam to the feed, pressure, temperature, and residence time in more detail. Catalyst development through the utilization of promoters and supports to improve activity and selectivity will be pursued.

INTRODUCTION

A number of processes for methane conversion to liquid hydrocarbons have been developed. Fox and coworkers (1990) compared the economics of several of these processes on a consistent design basis. The processes considered were:

- Non-Catalytic Partial Oxidation
- Oxidative Coupling
- Oxyhydrochlorination
- Fischer-Tropsch
- Fixed-Bed Methanol-to-Gasoline
- Fluid-Bed Methanol-to-Gasoline

The last three processes involve reforming methane to synthesis gas. The first three processes obtain liquids via direct methane conversion and are, therefore, potentially less expensive than processes involving reforming. Fox and coworkers (1990) found that fluid-bed methanol-to-gasoline (MTG) had the lowest overall cost, indicating that the direct conversion processes had not yet achieved a level of development allowing them to compete with reforming based technology. Furthermore, they found that selectivity and conversion per pass had the greatest effect on economics in the direct conversion processes. The most direct approach to improving conversion and selectivity in a partial oxidation process is to utilize a selective catalyst.

This conclusion is confirmed in a study by Hunter and coworkers (1990). They obtained high methanol selectivity at low conversion in a non-catalytic system. Their analysis indicates that improved conversion can only be obtained by increasing the oxygen content of the feed. To avoid dangerous, explosive conditions, this will require lowering the reaction temperature and pressure. For the reaction to proceed at an appreciable rate under these conditions, a catalyst is required.

The non-catalytic partial oxidation process relies on gas phase free-radical reactions to produce selective products. It seems likely that much higher yields

could be obtained using a catalytic system. By analogy to commercial processes for catalytic C_4 and C_3 hydrocarbon selective oxidation, a more ideal methane partial or selective oxidation system would operate in air at a low methane-to-oxygen ratio, high methane conversion, and high methanol yield. Because of the high methane conversion, no recycle is required. This approach eliminates both the oxygen production and reforming steps when compared to the conventional methanol synthesis flowsheet. It should be economically superior to the non-catalytic process described above because of the use of air rather than oxygen and the high methane conversion. Because of the relative simplicity of this process, it should be easily implemented in remote locations and on small scale.

Figure 1 illustrates two slightly different processes for direct catalytic oxidation of methane to methanol. The flow diagram shown in Figure 1 a) is the most ideal process and should have the lowest capital cost. Here air is used as the oxidant at low methane-to-oxygen molar feed ratio. High methane conversion is achieved with high selectivity for methanol. Because of the high conversion, there is no recycle. A preliminary cost analysis indicates that this process could be competitive with fixed-bed MTG if the yield of methanol obtained was higher than 42 percent (Morano, 1993).

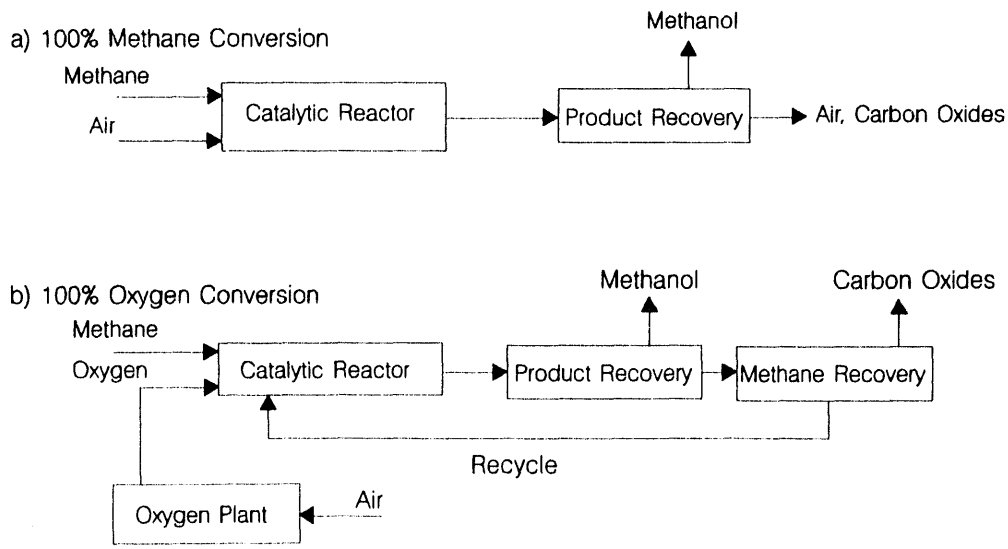

Figure 1. Simplified drawings of potential partial oxidation flowsheets.

A less ideal but probably more realistic scenario is shown in Figure 1 b). In this scheme, methane conversion is kept at intermediate or low levels (high CH_4:O_2 ratio) in order to achieve high methanol selectivity. The product recovery system is similar to that for the previous process but requires an additional methane recovery

and recycle step. Because of the low methane conversion and consequent high recycle, the use of oxygen rather than air is probably required. In much of the published work on methane partial oxidation, high methane-to-oxygen ratios were required for good selectivity to methanol or formaldehyde (Spencer and Pereira, 1987, 1989; Hunter et al., 1990). The key factor determining which of the process options shown in Figure 1 will be most economical is catalyst activity and selectivity.

CATALYTIC METHANE OXIDATION

Figure 2 shows an overall reaction pathway proposed for catalytic methane oxidation (Amiridis et al., 1991). This reaction network is based on the work of Spencer and Pereira (1987, 1989) using molybdenum and vanadium oxides. Their results indicate that methane reacts to form a surface intermediate (methoxy) which can desorb as methanol or react further to formaldehyde or carbon monoxide. Carbon monoxide formation was not observed directly from methane but only from formaldehyde. Carbon dioxide formation occurred primarily by direct oxidation of methane. Carbon monoxide can also be oxidized by the catalyst to form CO_2 or by reaction with water via the shift reaction.

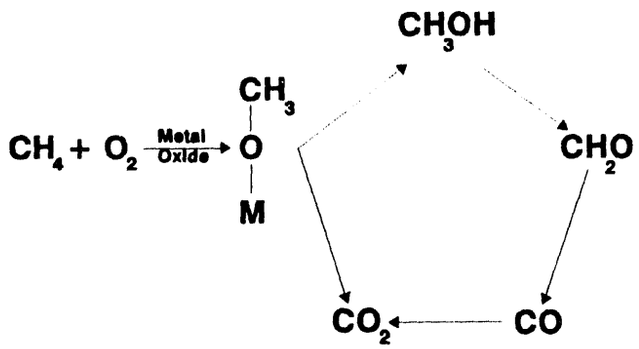

Figure 2. Overall reaction pathway proposed for methane oxidation (Amiridis et al., 1991).

The first step in methane oxidation is methane activation. Three possible routes of methane activation can be envisioned:

1. $CH_4 \rightarrow CH_3^- + H^+$
2. $CH_4 \rightarrow CH_3^{\cdot} + H^{\cdot}$
3. $CH_4 \rightarrow CH_3^+ + H^-$

Route 2 involves homolytic C-H bond cleavage to form radicals. Kung (1986) has compared Routes 1 and 2 based on calculated enthalpy of reaction. Based on his

results, Route 1 was rejected as being energetically unfavorable. Kung (1986) also concluded that alkane activation in general occurs via homolytic C-H bond cleavage.

The third route, H^- abstraction, has been suggested to occur over solid superacid catalysts (Pitchia and Klier, 1986). With these highly acidic materials, methane is protonated to form CH_5^+ which then reacts to form CH_3^+ attached to a surface oxygen. However, Hattori and coworkers (1981) observed that protonation of methane (and primary C-H bonds in general) does not occur over most solid superacids. Consequently, we conclude that Route 2, homolytic C-H bond cleavage to form radical intermediates, is the most important route of methane activation.

Figure 3 shows a possible surface reaction mechanism for methanol formation over a general metal oxide (MO_x). Most of the details of this mechanism are not well understood; however, some important features have begun to emerge. Methane is activated by formation of a surface methoxy group and a hydroxyl via the radical intermediates discussed above. Liu and coworkers (1984) suggest that methoxy formation occurs on a surface oxygen atom which is electron rich and may also be viewed as a basic surface site. Smith and Ozkan (1993) have also shown that M=O species are involved in selective methane oxidation to formaldehyde.

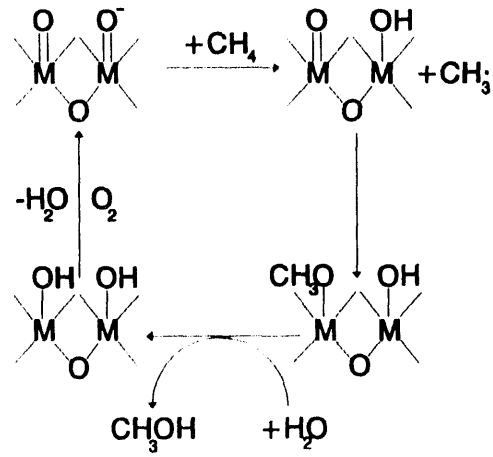

Figure 3. Surface reaction mechanism for methanol formation (after Lunsford, 1988).

The methoxy produced by methane adsorption on the basic surface can be further oxidized to formaldehyde and carbon oxides, or the methoxy can react with water or a surface hydroxyl to form methanol containing what was formerly a

surface lattice oxygen. The exact details of this recombination mechanism are not well understood. Several research groups have shown that steam in the feed gas can substantially enhance the selectivity to methanol over formaldehyde in methane oxidation. In particular, both Liu and coworkers (1984) and Khan and Somorjai (1985) observed that the rate of methanol formation was first order in steam partial pressure over molybdena catalysts with nitrous oxide as the oxidant. Liu and coworkers have also shown that the formation of methanol by reaction of molybdenum methoxide and water is extremely facile. Within the context of the recombination mechanism, a significant partial pressure of steam in the reaction mixture could lead to enhanced concentration of surface hydroxyls and an enhanced rate of recombination to form methanol.

Based on these mechanistic considerations, the catalyst properties required for selective oxidation of methane to methanol should include:

- Basic sites for methane activation.
- M=O groups for methoxy group formation.
- Reactive or acidic surface hydroxyls to insure methanol formation.

Vanadium phosphate catalysts have these properties and may, therefore, have the potential to selectively oxidize methane to methanol. In particular, VPO catalysts are well known to activate alkanes and possess a dual acid/base site.

SELECTIVE OXIDATION WITH VANADIUM PHOSPHATE

The primary commercial use of VPO catalysts is in C_4 hydrocarbon oxidation to maleic anhydride. Vanadium phosphates have also shown good selectivity for oxidation of ethane to ethylene (Michalakos et al., 1993). The catalytic oxidation is generally performed at 350 to 500°C, near atmospheric pressure, using 1 - 2 percent butane in air. Conversion near 90 percent and selectivity to maleic anhydride of 60 - 70 percent are reported (Hodnett, 1985).

The butane oxidation mechanism has been shown to consist of a number of steps, including butane activation, dehydrogenation, oxygen insertion, product desorption, and catalyst reoxidation. There is disagreement as to whether the rate determining step is butane activation (removal of a methyl or methylene hydrogen) or concerted water desorption and catalyst reoxidation.

The active and selective component of the catalyst is thought to be vanadyl pyrophosphate. This phase has been shown to contain strong Lewis and Bronsted acid sites as well as Lewis base sites (Busca et al., 1986). A high concentration of highly mobile surface hydroxyl groups is also present (Pepera et al., 1985). These acidic and basic sites, as well as a surface vanadyl (V=O), make up the active site ensemble shown in Figure 4. This active site contains all of the elements proposed above for an active and selective methane oxidation catalyst. Given these

properties and the known ability of this catalyst to activate alkanes, it was selected for testing in methane oxidation.

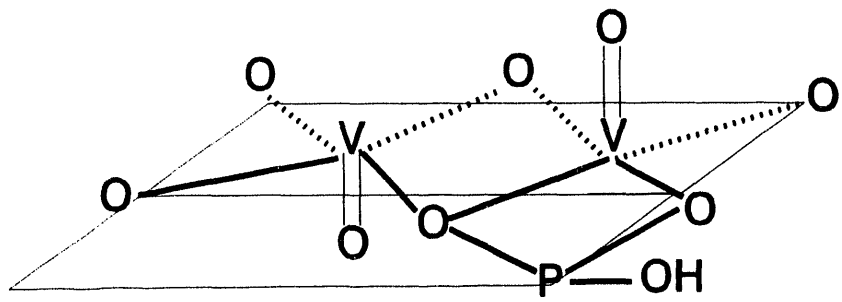

Figure 4. Active site proposed for VPO catalysts in C_4 oxidation (Busca et al., 1986).

RESULTS AND DISCUSSION

Experimentally our work involves catalyst preparation and activation, catalyst characterization, and catalyst testing. The first phase of the program has involved preparation and testing of unmodified VPO catalysts in methane oxidation. This work is described below.

CATALYST SYNTHESIS AND ACTIVATION

VPO catalyst synthesis involves contacting V_2O_5 with aqueous acid or an organic alcohol under reflux conditions. A portion of the vanadium is reduced to the +4 oxidation state. The slurry is then cooled and phosphoric acid is added. This mixture is then refluxed for an additional length of time wherein the remaining vanadium becomes reduced and the catalyst precursor $VO(HPO_4)\bullet 0.5H_2O$ is formed. The precursor is recovered by filtration or evaporation of the liquid. A very large number of variations on this basic method are described in the patent and scientific literature.

Catalyst synthesis is conducted in a 500 ml, glass, round bottom, three-necked flask. The flask is equipped with a reflux condenser on neck one and a teflon impeller-shaft assembly on neck two. For some of the preparations, a Dean-Stark trap was used with the reflux condenser to remove water from the refluxing slurry. The third neck is used for reagent addition. The flask is heated with an electric resistance heating mantle. The preparations which have been prepared so far can be divided into three general types:

- Aqueous Two-Stage Preparation

  Fifteen grams of V_2O_5 was dissolved in 37 percent aqueous HCl. The solution was stirred and refluxed for 3 hours. Phosphoric acid (22.8 grams) was then added, yielding a P:V ratio of 1.2, and refluxing was continued for another 2 hours. The solution was poured into a beaker and water was evaporated overnight at 150°C, yielding a light blue solid. This blue solid was then washed in boiling water for 1 hour and air dried at 150°C for 24 hours.

- Organic Two-Stage Preparation

  Fifteen grams of V_2O_5 was suspended in 90 ml of isobutyl alcohol and 60 ml of benzyl alcohol. The suspension was stirred and refluxed for 3 hours, then cooled overnight with stirring before the addition of 24.5 grams of 85 percent ortho-H_3PO_4. This yielded a P:V ratio of 1.3. After phosphorus addition, the solution was heated and refluxed for 2 hours. The resulting slurry was filtered, washed with water, and dried (150°C for 24 hours), yielding a light blue precursor.

- Organic One-Stage Preparation

  Fifteen grams of V_2O_5 and 19.58 grams of 99 percent ortho-H_3PO_4 were added to 90 ml of isobutyl alcohol and 60 ml of benzyl alcohol. This yielded a starting P:V ratio of 1.2. This slurry was then refluxed for 6 hours before cooling overnight, filtering, and washing with a fresh isobutyl/benzyl mixture. The light blue precursor was dried at 150°C for 5 hours.

X-ray powder diffraction patterns for catalyst precursors prepared using these methods are shown in Figure 5. For the aqueous preparation, two patterns are shown, before and after water washing. Analysis of the peaks indicates that before water washing, this sample is roughly 50 percent $VO(HPO_4)$-$0.5H_2O$ (Johnson et al., 1984), the desired precursor phase. The sample also contains a significant amount of $VO(H_2PO_4)_2$ and other unidentified phases. Washing of this sample in boiling water effectively removes the peaks of $VO(H_2PO_4)_2$ and the other unidentified phases, leaving only the desired phase. Peaks in both of these samples are very sharp, indicating a high degree of crystallinity. For the washed sample, all of the reported peaks of the precursor compound were observed.

Powder diffraction patterns for precursors produced by non-aqueous methods are also shown in Figure 5. The predominant phase observed is $VO(HPO_4)\bullet 0.5H_2O$ for all samples, although relative intensities differ slightly from those reported by Johnson and coworkers (1984). When compared to the aqueous preparation, much broader peaks are observed and some of the lower intensity peaks are missing. This is consistent with the reported lower crystallinity of non-aqueous precursors and their distinctly different crystal face development (Hutchings, 1991).

An additional phase is observed at low levels for the single-stage organic preparation. The d values correspond to those reported for $VO(H_2PO_4)_2$. Presumably the single stage procedure is responsible for the formation of the undesired material. Two-stage preparations in either organic or aqueous media appear to be suitable for preparing the precursor as long as the aqueous precursor is washed in boiling water. However, several investigators have noted that there is a significant difference in the activity and selectivity of the aqueous and organic preparations in butane oxidation (Hutchings, 1991). Organic preparations are much more active and selective. This is thought to be related to the different crystal face exposure that results from the preparation conditions.

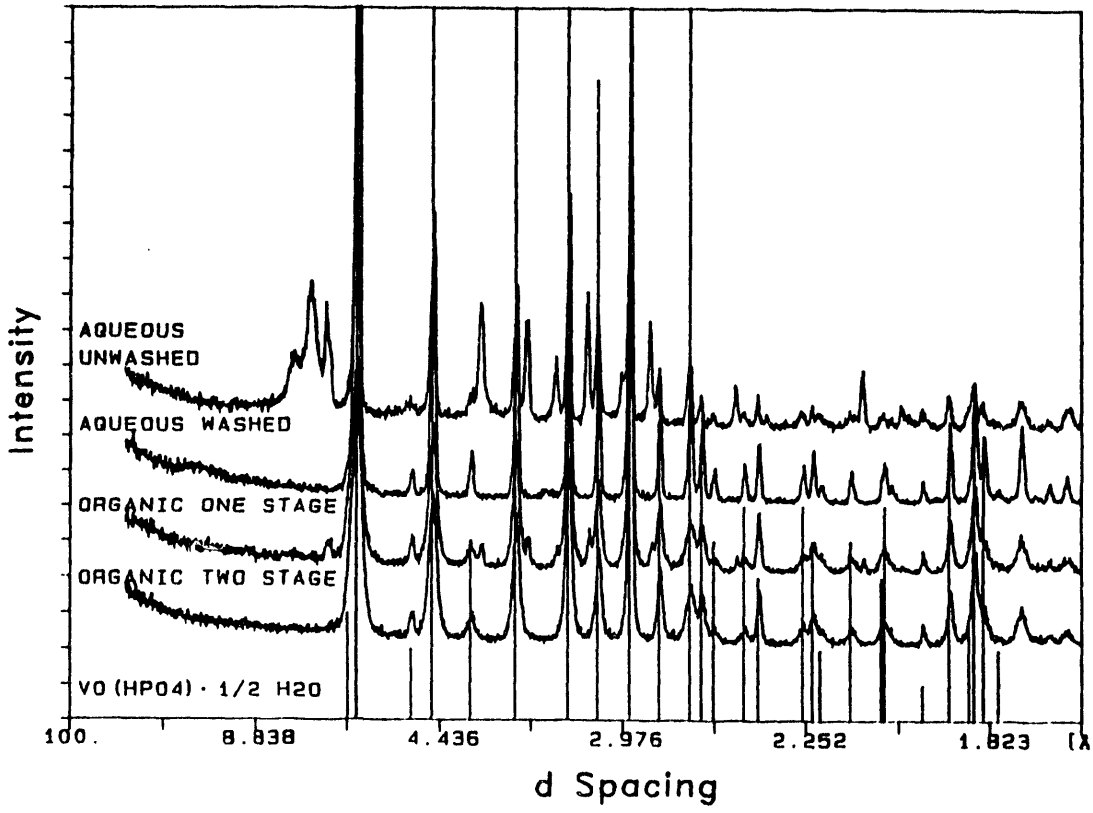

Figure 5. X-ray powder diffraction patterns for catalyst precursors.

CATALYST ACTIVATION

There is much experimental evidence that activation of the precursor to form the active catalyst is a critical step in VPO catalyst preparation (Hodnett, 1985; Arnold and Sundaresan, 1988). Activation is typically carried out by first heating the precursor at 3°C/minute in air to 380°C and holding for 2 or more hours. A

reaction gas environment (1 percent butane in air for maleic anhydride catalysts) is then introduced and the catalyst is heated at 3°C/minute to temperatures as high as 500°C. During activation, a topotactic transformation of $VO(HPO_4)$-$0.5H_2O$ to $(VO)_2P_2O_7$ occurs (Johnson et al., 1984). A large number of variations on this basic procedure are reported in the patent and academic literature. For example, activation in hydrogen and nitrogen has been performed successfully. Heating rate can affect activation results. Steam has been shown to accelerate activation (Arnold and Sundaresan, 1988).

Optimal activation conditions for methane oxidation catalysts have not been determined. We are testing several different procedures and evaluating the results using X-ray diffraction and methane oxidation testing. A good activation procedure should generate the X-ray diffraction pattern of $(VO_2)P_2O_7$ or the patented B-phase which is very similar to $(VO_2)P_2O_7$ (Schneider, 1975).

Activation was carried out in a temperature programmable tube furnace under various flowing gas environments and for varying lengths of time as described below. Small porcelain boats were filled with precursor and inserted into the furnace cold. Several representative activation procedures are listed below.

1. Heating in N_2/500°C

   The sample was heated to 500°C at 5°C/minute under nitrogen and held for 24 hours.

2. Heating in Air/400°C

   The sample was heated to 400°C at 3°C/minute in air and held at that temperature for 24 hours.

3. Programmed Heating Air/380°C-N_2/480°C

   The sample was heated in air at 3°C/minute to 380°C and held for 2 hours. The gas was switched to nitrogen and the sample was heated at 3°C/minute to 480°C and held for 16 hours.

4. Programmed Heating Air/380°C-Wet N_2/500°C

   The sample was heated in air to 380°C at 3°C/minute and held 4 hours. The gas was then switched to nitrogen which was passed through a bubbler where it was saturated with moisture. The temperature was increased to 500°C at 3°C/minute and held for 16 hours.

Activated catalysts were characterized by X-ray powder diffraction, measurement of P:V ratio, and BET surface area. X-ray powder diffraction patterns

for various activated samples are shown in Figure 6 for a precursor prepared in organic media. Activation using Procedure 1 produces a pattern very similar to that reported for the active B-phase in the patent literature (Horowitz et al., 1988; Schneider, 1975) and exhibits the strongest peaks of $(VO)_2P_2O_7$. Note that the patented B-phase and $(VO)_2P_2O_7$ yield very similar powder patterns but several peaks are absent for the B-phase. Some researchers consider the B-phase to be a mixture of $(VO)_2P_2O_7$ and structurally closely related phases. Activation 2 yields a more intense pattern which matches that of $(VO)_2P_2O_7$. Activation 3 produces a pattern similar to that of $(VO)_2P_2O_7$; however, intensities are highly skewed, suggesting that the transformation is incomplete. Exposure to these activation conditions for a longer time might yield the desired phase. Activation 4 in wet nitrogen leads to a more highly crystalline sample of $(VO)_2P_2O_7$. This XRD pattern is thought to be more representative of equilibrium VPO catalysts which exhibit improved selectivity after several hundred hours on stream (Cornaglia et al., 1991).

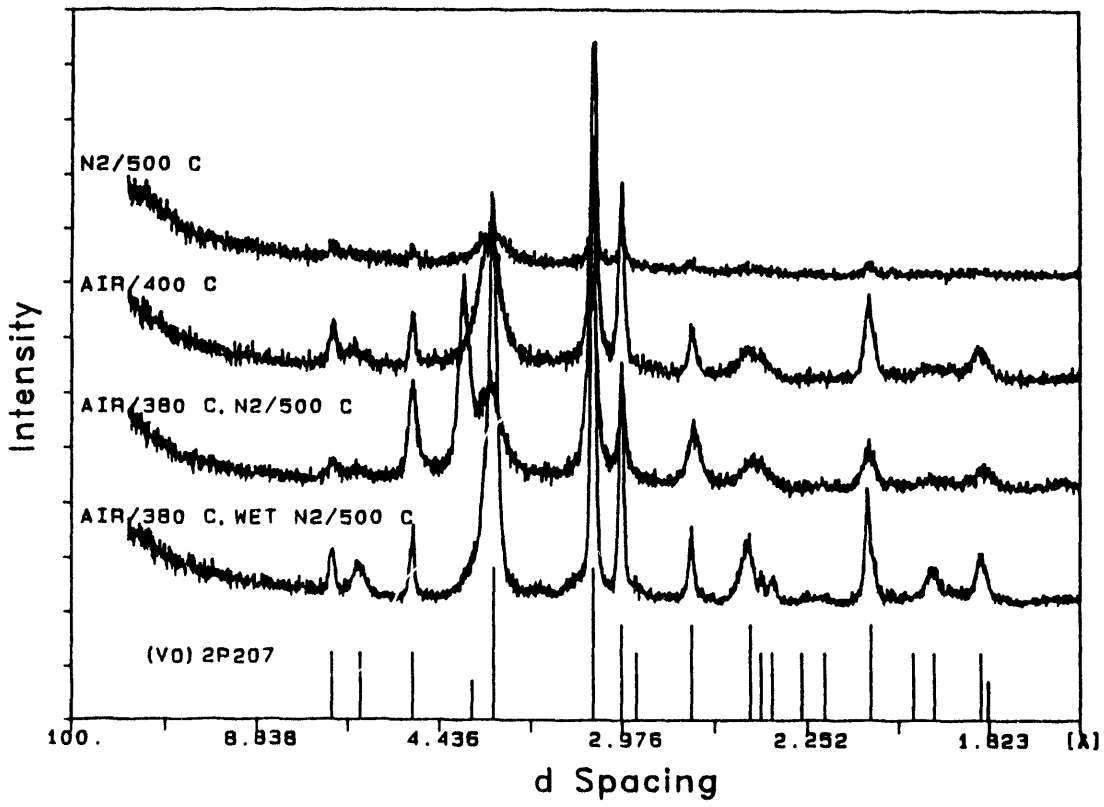

Figure 6. X-ray diffraction patterns for activated samples.

Table 1 lists P:V ratios and surface areas for precursors and activated samples. Replicate P:V determinations on one sample produced the values of 1.05,

1.01, 1.00, 1.03, 1.00, 1.04, and 1.02, for an average of 1.02 with standard deviation of 0.020. Given this level of analytical variability, the apparent changes observed in the P:V ratio upon activation are not significant in most cases. However, activation in steam may have significantly reduced the P:V ratio. A step change in selectivity for C_4 oxidation occurs upon increasing the P:V ratio from slightly less than 1 to slightly greater than 1 with P:V greater than 1 required for high selectivity (Hodnett, 1985). Therefore, steam activation may not be the optimum procedure, although highly selective catalysts have been reported using steam (Arnold and Sundaresen, 1988). Surface areas of the activated catalysts are generally in the range of 15 to 20 m^2/g. However, activation method 1 yields catalysts with a higher surface area (27 m^2/g).

Table 1. P:V Ratios and Surface Areas for Activated Catalysts (Organic Two-Stage Preparation)

Activation Method	Precursor P:V	Activated P:V	Surface Area, m^2/g
1	1.02	0.99	27
2	1.02	1.01	23
2	1.02	1.01	22
3	1.02	1.02	16
3	1.02	1.00	15
4	1.02	0.97	18

These activation results reveal a very complex interaction between activation time, temperature, and gas environment. The best results are obtained by holding at a temperature of 400°C or lower in any gas environment before going to higher temperatures. Non-oxidizing gas environments are preferred for the higher temperature treatments. In dry gas environments, XRD patterns contain all of the peaks of $(VO)_2P_2O_7$, but intensities are skewed suggesting that the solid state transformation is incomplete. Activation in wet gas yields a completely transformed sample in the same length of time. Based on these considerations, activation by heating in air to 400°C for several hours followed by heating to higher temperatures in wet nitrogen was employed for the test work presented in this paper. Given the reduced P:V observed for these samples, future work will include testing of catalysts activated in dry conditions to have P:V greater than 1.

CATALYST TESTING

Catalysts are tested in a small fixed-bed reactor system. The system includes mass flow controllers which meter gases into a back pressured manifold. Gases

from the manifold flow directly to a feed gas sampling valve and the reactor. Steam can be added to the feed gas in one of two ways. At near atmospheric pressure, the gas is bubbled through a saturator which can be heated to a controlled temperature, or at elevated pressure, the gas is routed to a steam generator which is heated by an electric resistance heating element. Water is supplied to the steam generator from an Eldex metering pump. Steam-containing gas mixtures flow from the steam generator to the feed gas sampling valve and then to the reactor inlet.

Gases flow through the small fixed bed in up flow. The reactor itself consists of a 0.5-inch stainless steel tube inside of which is a thick walled quartz tube liner (4 mm i.d.). The liner is cemented into the steel tube to prevent flow bypassing. The catalyst bed is preceded by a zone packed with quartz chips. The catalyst bed is usually 0.4 to 1 gram of 0.8 by 1.4 mm catalyst particles. The aft zone of the reactor is also packed with quartz chips. A thermocouple extends from the reactor inlet to the bottom of the catalyst bed providing a measure of bed inlet temperature. The reactor is heated with an electric furnace. A thermocouple near the furnace elements is used as input to the temperature controller. Reactor pressure is controlled by a back pressure regulator. Gases flowing from the reactor pass through a sampling valve to the GC. All transfer tubing and sample lines are heated to 150°C with heating tape and insulated.

Gas analysis is accomplished with a Hewlett-Packard 5890A gas chromatograph coupled with a 3396A integrator. Helium is used as the carrier gas and purified to remove traces of moisture and oxygen. The GC is equipped with a gas sampling/flow reversal valve and a column isolation valve. Separation of product gases is accomplished with using two columns. A Chromosorb 107 column is used to separate formaldehyde, water, and methanol. A Carbosphere column is used for separation of oxygen, carbon monoxide, methane, and carbon dioxide. Gases are detected with a thermal conductivity detector.

The performance of this reactor system was verified by reproducing data reported in the literature for methane partial oxidation to formaldehyde over V_2O_5/SiO_2 (1 weight percent V). The results shown in Figure 7 were obtained. This plot shows formaldehyde selectivity as a function of methane conversion at temperatures near 575°C. Our results are seen to be in agreement with those of Spencer and Pereira (1989) and Koranne and coworkers (1992), confirming the performance of our reactor and analytical systems.

VPO catalysts prepared in organic and aqueous media and activated in steam/nitrogen to produce highly crystalline $(VO)_2P_2O_7$ were tested. The reaction gas was 93 percent methane/balance oxygen. Results are listed in Table 2 for the organic media catalyst (VPO_{org}) and in Table 3 for the aqueous HCl catalyst (VPO_{aq}). Oxygen conversion was less than 100 percent in all cases. Carbon oxides are the only products observed under these conditions.

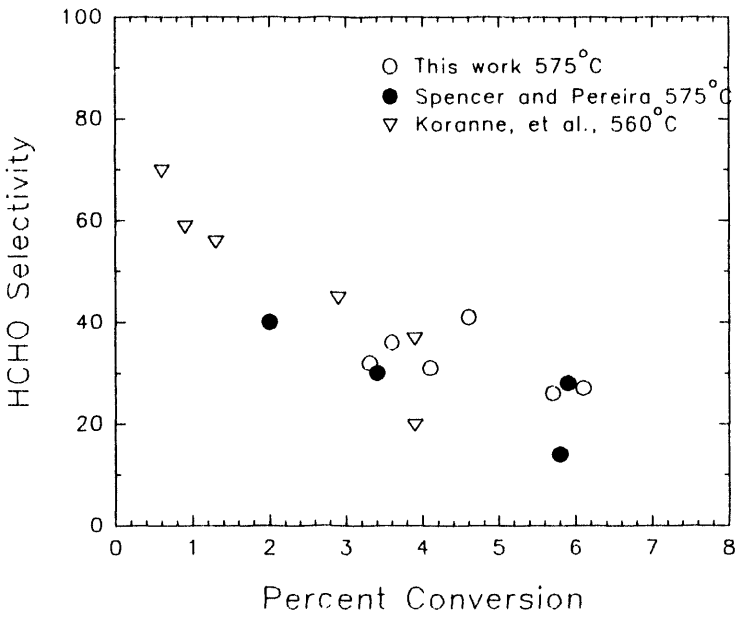

Figure 7. Formaldehyde selectivity as a function of methane conversion for vanadia/silica catalyst.

Table 2. Results of Methane Oxidation Run Using $(VO)_2P_2O_7$ Prepared in Organic Media

Nominal Temperature, °C	Pseudo-Contact Time, mg-min/ml	% CH_4 In.	% Conversion	% Selectivity CO	% Selectivity CO_2
450	8	88	1.78	97	3
450	12	93	1.19	95	5
475	12	93	2.17	95	5
500	3	93	0.34	100	0
500	7	93	0.82	100	0
500	12	92	3.80	94	6
525	5	93	2.57	96	4
550	12	93	5.39	90	10
575	12	93	7.72	89	11

Table 3. Results of Methane Oxidation Run Using $(VO)_2P_2O_7$ Prepared in Aqueous HCl

Nominal Temperature, °C	Pseudo-Contact Time, mg-min/ml	% CH_4 In.	% Conversion	% Selectivity CO	% Selectivity CO_2
450	12	93	0.12	66	34
475	12	93	0.40	66	34
500	12	93	0.57	73	27
550	12	93	2.35	47	53

The VPO_{org} catalyst was more active than VPO_{aq} or V_2O_5/SiO_2, as shown in Figure 8 where conversion is plotted as a function of temperature under otherwise identical conditions. Results for blank runs are also included and indicate that homogeneous conversion of methane is very low. It should be noted that the surface area of the silica supported catalyst is 160 m^2/g, while that of the VPO catalysts is about 20 m^2/g.

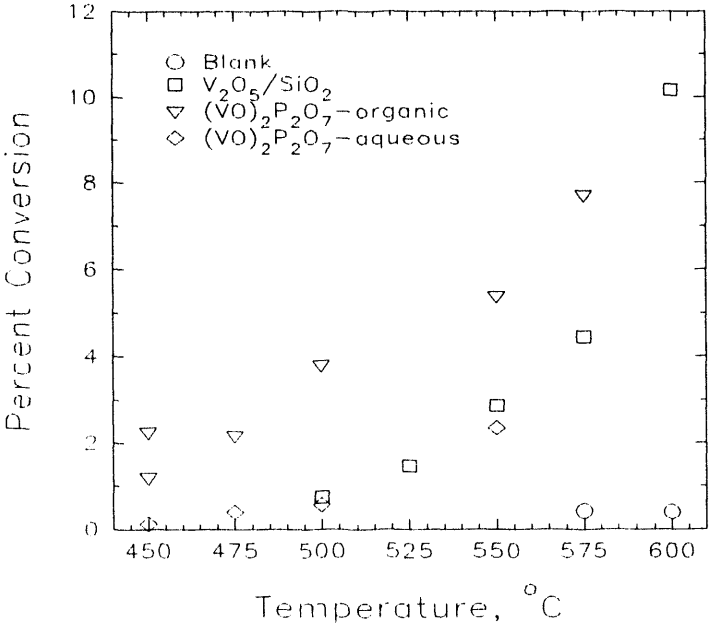

Figure 8. Conversion as a function of temperature for methane oxidation over VPO and V_2O_5/SiO_2 catalysts at 1 atm, 93 percent CH_4, and 12 mg-min/ml pseudo-contact time.

Carbon monoxide selectivity as a function of temperature is plotted in Figure 9 for these catalysts. The VPO_{org} catalyst produces almost exclusively CO, while considerable CO_2 is observed over VPO_{aq} and V_2O_5/SiO_2. Referring to the reaction pathway shown in Figure 2, this high CO selectivity suggests that a reaction pathway which includes selective intermediates is operative on VPO_{org}. Alteration of reaction conditions or promotion of the catalyst might, therefore, allow these selective products to be observed in the product gas. Also, the P:V ratio of this catalyst is 0.97 and selectivity in C_4 oxidation is dramatically lower when the P:V ratio is less than 1.

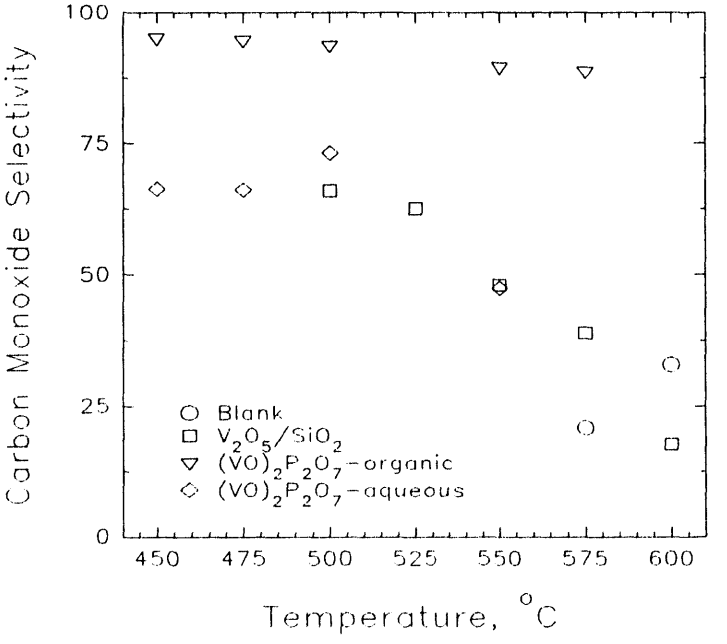

Figure 9. Carbon monoxide selectivity as a function of temperature for various catalysts, reaction conditions as in Figure 8.

Figure 10 shows XRD results for the fresh VPO_{org} catalyst and for a sample removed from the reactor after testing at temperatures up to 575°C. The patterns are very nearly identical and both correspond to $(VO)_2P_2O_7$. Recently acquired XRD results for the used VPO_{aq} catalyst indicate that it had transformed to β-$VOPO_4$ which is not known to be a selective catalyst.

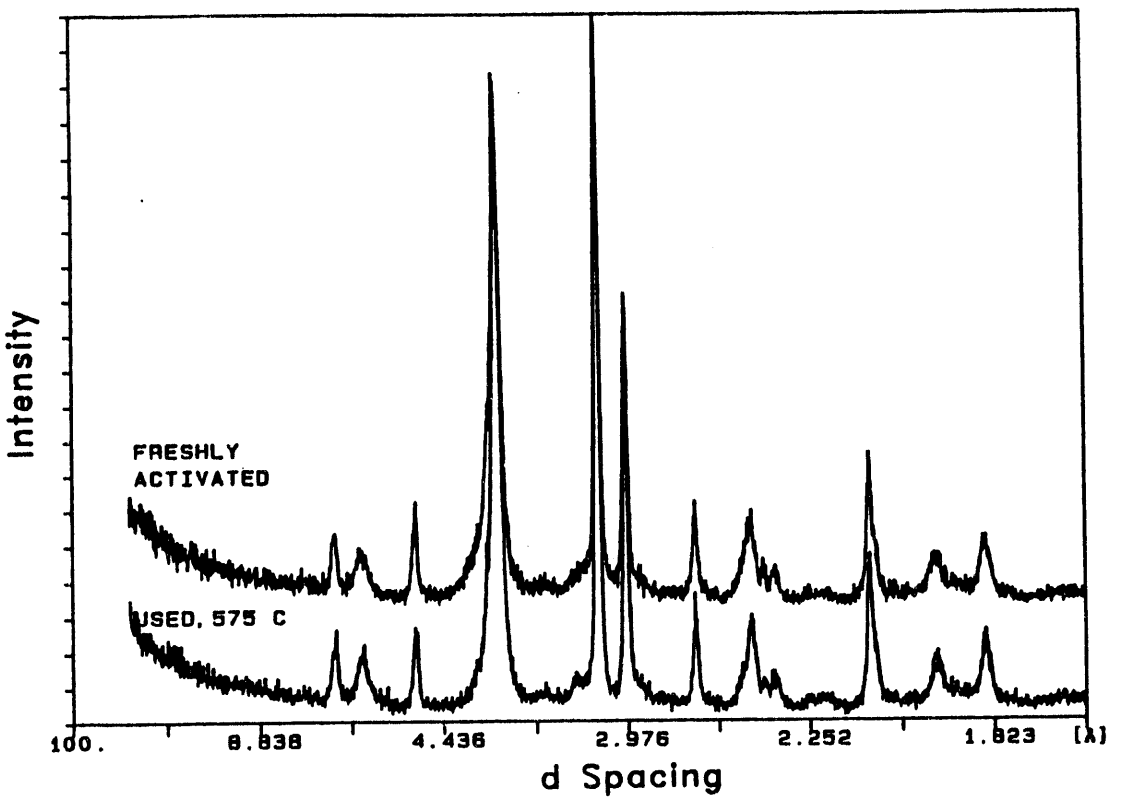

Figure 10. XRD patterns for fresh and used (575°C) VPO_{org} catalysts.

CONCLUSIONS AND RECOMMENDATIONS

The most important conclusion that can be drawn from work on this program to date is that, for the catalysts and reaction conditions tested, VPO_{org} is highly active but exhibits no selectivity for methanol or formaldehyde. Preparation of a catalyst using the same conditions but with a higher P:V ratio might lead to the formation of more selective products. Selectivity to carbon monoxide was above 90 percent under most reaction conditions. This suggests that different reaction conditions or modification of the catalyst to prevent over oxidation could lead to the formation of selective products. The VPO_{aq} catalyst exhibits an activity level similar to that of V_2O_5/SiO_2. However, CO_2 and CO were the only products observed. The VPO_{org} catalyst was shown to be stable under high methane/oxygen ratio reaction conditions. The VPO_{aq} catalyst was not stable, being transformed to a more oxidized phase.

The process variable study will be expanded in the future to include more data on the effect of the following variables:

- CH_4/O_2 Ratio
- CH_4/H_2O Ratio
- Pressure
- Temperature
- Residence Time
- Catalyst Preparation and Activation Conditions

Conditions where complete oxygen consumption is obtained will be investigated. Also, the effect of low levels C_2 and C_3 hydrocarbons in the feed will be examined. This data will be used to select a narrow range of conditions for testing of promoters and supports.

The second phase of this project involves improving the basic VPO catalyst through the use of promoters and supports. Given the high activity of the catalyst in methane oxidation, work with promoters and supports will be directed at improving selectivity. A large number of modifiers and promoters for VPO catalysts used in C_4 oxidation have been described in the patent literature. The use of Ba, Ce, Co, Cr, Cu, Fe, K, La, Li, Mg, Mn, Mo, Si, SO_4^{2-}, Ti, Te, U, W, Zn, and Zr are noted in the reviews by Hodnett (1985) and Hutchings (1991). Patented catalysts are frequently promoted by more than one element. These promoters can substantially lower the temperature required for C_4 oxidation and improve activity and selectivity.

The mechanism through which most promoters function is not well understood. However, the action of several promoters has been studied in some detail, and this information, combined with the preliminary reactivity results described above, can be used to select several elements for testing. Because the VPO_{org} catalyst produces CO rather than less oxidized products, promoters which reduce oxygen reactivity or promote desorption of less oxidized products are desired. Cobalt, molybdenum, and zinc are known to increase the surface oxidation state of VPO catalysts and reduce oxygen reactivity (Hutchings, 1991; Varma and Saraf, 1979). Cobalt and Mo are utilized at low loadings (Co or Mo/V molar ratio of 0.02). Zinc is utilized at higher loadings near 5 weight percent and forms a separate zinc oxide phase (Takita et al., 1991). These promoters will be tested in future work.

Transition metal oxide catalysts interact strongly with oxide catalyst supports, and this interaction can have a great effect on catalytic activity (Connell and Dumesic, 1987; Deo and Wachs, 1991). VPO catalysts are usually used without a support in butane oxidation, so only limited information on support effects is available. However, it has been shown that the support can affect activity and selectivity in C_4 oxidation (Kuo and Yang, 1989; Centi et al., 1984). Aluminum phosphate, titania, and HY zeolite have shown the potential to improve selectivity and decrease the reducibility of VPO. These supports, along with silica and magnesia, will be tested.

The test work outlined above will allow a thorough evaluation of the potential of vanadium phosphates as methane selective oxidation catalysts.

REFERENCES

Amiridis, M. D., Rekoske, J. E., Dumesic, J. A., Rudd, D. F., Spencer, N. D., and Pereira, C. J., AIChE J. 37 87 (1991).

Arnold, E. W. and Sundaresan, S., Appl. Catal. 41 225 (1988).

Busca, G., Centi, G., and Trifiro, F., Appl. Catal. 25 265 (1986).

Centi, G., Jiru, P., and Trifiro, F., Successful Design of Catalysts, Elsevier, Amsterdam, 1988, pp. 247.

Connell, G. and Dumesic, J. A., J. Catal. 105 285 (1987).

Cornaglia, L. M., Caspani, C., and Lombardo, E. A., Appl. Catal. 74 15 (1991).

Deo, G. and Wachs, I. E., J. Catal. 129 307 (1991).

Fox, J. M., III, Chen, T.-P., and Degen, B. D., Chem. Eng. Prog. (4) 42 (1990).

Hattori, H., Takahashi, O., Takagi, M., and Tanabe, K., J. Catal. 68 132 (1981).

Hodnett, B. K., Catal. Rev. Sci. Eng. 27 373 (1985) and references therein.

Horowitz, H. S., Blackstone, C. M., Sleight, A. W., and Teufer, G., Appl. Catal. 38 193 (1988).

Hunter, N. R., Gesser, H. D., Morton, L. A., Yarlagadda, P. S., and Fung, D. P. C., Appl. Catal. 57 45 (1990).

Hutchings, G. J., Appl. Catal. 72 1 (1991).

Johnson, J. W., Johston, D. C., Jacobson, A. J., and Brody, J. F., J. Am. Chem. Soc. 106 8123 (1984).

Khan, M. M. and Somorjai, G. A., J. Catal. 91 263 (1985).

Koranne, M. M., Goodwin, J. G., Jr., and Marcelin, G. ACS Div. Petr. Chem. Prepr. 37 (1) 41 (1992).

Kung, H. H., Ind. Eng. Chem. Prod. Res. Dev. 25 171 (1986).

Kuo, P. S. and Yang, B. L., J. Catal. 117 301 (1989).

Liu, H. F., Liu, R. S., Liew, K. Y., Johnson, R. E., and Lunsford, J. H., J. Am. Chem. Soc. 106 4117 (1984).

Lunsford, J., ACS Div. Fuel Chem. Prepr. 33 (3) 357 (1988).

Michalakos, P. M., Kung, M. C., Jahan, I., and Kung, H. H., J. Catal. 140 226 (1993).

Morano, J., Burns and Roe Services, private communication (1993).

Pepera, M. A., Callahan, J. L., Desmons, M. J., Milberger, E. L., Blum, P. R., and Bremer, N. J., J. Am. Chem. Soc. 107 4883 (1985).

Pitchai, R. and Klier, K., Catal. Rev.-Sci. Eng. 28 13 (1986).

Schneider, R. A., United States Patent No. 3,864,280, February 4, 1975.

Smith, M. R. and Ozkan, U. S., J. Catal. 141 124 (1993).

Spencer, N. D. and Pereira, C. J., AIChE J. 33 1808 (1987).

Spencer, N. D. and Pereira, C. J., J. Catal. 116 399 (1989).

Takita, Y., Tanaka, K., Ichimaru, S., Ishihara, T., Inoue, T., and Hiromichi, A., J. Catal. 130 347 (1991).

Varma, R. L. and Saraf, D. N., Ind. Eng. Chem. Prod. Res. Dev. 18 7 (1979).

DIRECT AROMATIZATION OF METHANE

Contract No. DE-22AC-92PC92109

George Marcelin, Rachid Oukaci, and Ruben A. Migone

Altamira Instruments, Inc.
2090 William Pitt Way
Pittsburgh, PA 15238

ABSTRACT

The last decade has seen increased efforts in research aimed at converting natural gas directly into value added products. Most of this research has been aimed at the catalytic oxidative coupling of methane to ethane/ethylene or at the partial oxidation to form methanol/formaldehyde. In both instances the reaction yields the partially oxidized products as well as a significant amount of total oxidation products, i.e. CO and CO_2.

Methane can also be activated by thermal means. Pyrolysis of methane is a suitable method of producing higher molecular weight homologs, in particular aromatics compounds. The main disadvantage of current pyrolytic methane conversion schemes is that significant amounts of solid coke are formed as a byproduct of the reaction. This coke byproduct can be minimized by employing a reactor design that quenches the reaction prior to the onset of solid carbon formation. This project involves an investigation of novel pyrolytic means of directly converting methane into aromatic products with minimum formation of solid carbon by use of a novel reactor designed to rapidly quench the free-radical combustion reaction so as to maximize the yield of aromatics.

INTRODUCTION

Significant amounts of natural gas (mainly methane) exist worldwide and prospects are good for maintaining secure, reliable, and adequate supplies at competitive prices well into the future. Approximately 6% of the estimated 3,500 trillion cubic feet of worldwide proven natural gas are found in the US (Sperling, 1989). This carbon source is produced concurrently with crude oil and is also a significant product in coal gasification and indirect

liquefaction processes. Because of transportation problems, most natural gas is flared at the source after natural gas liquids are extracted; wasting this valuable resource and allowing the release of uncombusted natural gas and vast quantities of carbon dioxide into the atmosphere.

Processes exist for utilizing natural gas. Liquefication can be employed as a method of transportation but processes for liquefying, transporting, and revaporizing natural gas are complex, energy-intensive, and require extensive safety precautions (Leibson, 1987). Liquefaction via synthesis gas can be used to produce methanol or hydrocarbons but involves large capital expenditures (King, 1981).

The last decade has seen an increased effort in research aimed at converting natural gas directly into value added products. Most of this research has been aimed at the catalytic oxidative coupling of methane to ethane/ethylene (Keller, 1982; Driscoll, 1985; Otsuka, 1985; Agarwal, 1986) or at the partial oxidation to form methanol/formaldehyde (Pitchai, 1986). In both instances the reaction yields the partially oxidized products as well as a significant amount of total oxidation products, i.e. CO and CO_2.

One troubling limitation of these reactions is the fact that the products are more easily oxidized than the reactant and thus it is difficult to produce high yields of the desired partial oxidation products. McCarty and co-workers (Quinian, 1988) first suggested that a barrier of about 25 mole% existed to the yield of higher hydrocarbons in the oxidative coupling of methane.

Methane can also be activated by thermal means. Thermal activation leading to acetylene has been practiced commercially for decades (Wiessermel, 1978). This reaction occurs at about 1400°C, and reports exist of reaction at lower temperatures leading to aromatics (Sanchez, 1966; Friedman, 1970). Combination of oxidative coupling reactors and pyrolytic reactors have also been reported as a means for achieving higher homologs than usually formed in just the oxidative coupling reaction (Mimoun, 1989).

Pyrolytic means to methane conversion has a number of advantages over catalytic partial oxidation. Firstly, because it is carried out in the absence of oxygen, the yield barrier suggested by McCarty no longer exists. Secondly, pyrolysis is capable of producing higher molecular weight homologs, in particular aromatics, which are easier to transport and have high value as a petrochemical feedstock. Thirdly, it produces hydrogen as a byproduct which

is commercially valuable. The main disadvantage of current pyrolytic methane conversion schemes is the formation of significant amounts of solid coke as byproducts of the reaction.

Methane pyrolysis proceeds through a recursive free radical mechanism to produce traditional unsaturated chemical and refining feedstocks, such as ethylene and benzene, and has received much attention because of its inherent simplicity. However, successful processes have not been demonstrated due to the high temperature required to activate methane, which results predominantly in acetylene and/or carbon, with low yields of useful hydrocarbons. Some examples of pyrolysis techniques include the Wulff or Huls process, where methane is pyrolyzed at high temperatures ($>1200^{o}C$) in a regenerative furnace or electric arc to produce acetylene, hydrogen, carbon black, and traces of di- and triacetylene as well as controlled systems that produce diamonds and carbon fibers (Deryaguin, 1973; Murata, 1989).

The pyrolysis of methane can be considered to follow a step dehydrogenation sequence:

$$2CH_4 \text{ ---> } C_2H_4 \text{ ---> } C_2H_2 \text{ ---> } 2C$$

to produce, by free radical mechanisms, higher unsaturated hydrocarbons, aromatics, and eventually carbon. Thermodynamic equilibrium calculations can show the driving force of the reaction to be toward solid carbon. Indeed, any combination of reaction temperature and throughput which achieves appreciable methane utilization ($>10\%$) also results in solid carbon and hydrogen as the principal equilibrium products (Khan, 1970).

The growth of stable, unsaturated hydrocarbon products can be considered a non-chain process. Methyl and/or methylene radicals react during the reaction producing stable cyclic molecular species. The principal radical reaction pathways to products are through combinations, disproportionations, and additions/abstraction with other molecules. Such pathways have rather low activation energies, <15 kcal/mole, in comparison to the primary decompositions. The radical or hydrocarbon termination step is the formation of solid carbon. It is quite complex, probably autocatalytic, and involves the formation of polyunsaturated and polyaromatic hydrocarbons and their eventual condensation and dehydrogenation to solid carbon. Markarov and Pechkik (1974) found the energy of activation for this termination step to be about 17 kcal/mole larger than radical propagations to hydrocarbons. Two problem areas can be identified which lead to the

formation of solid carbon during the pyrolysis of methane. The first is reactor contact time. Makarov and Pechik (1974), working at temperatures less than 1100°C, found that at contact times less than a second solid carbon formation was negligible and hydrocarbon yields were a maximum. Also, the rate of carbon formation during methane pyrolysis increased proportionately with contact time and the lower the reactor surface/volume ratio the sharper the increase of the rate and the higher its value.

A second problem area is the mechanism of carbon formation through polyaromatic intermediates (Lieberman, 1973; Oro, 1966; Prado, 1978). These can be addressed by limiting the reaction of the intermediates by removing them from the reaction zone before they can be converted to coke. BP has disclosed an integrated process for the production of liquid hydrocarbons from methane which consists of first pyrolyzing the methane, followed by quenching the effluent with water and liquid hydrocarbons so as to condense all condensable components and effect separation (Brophy, 1987).

Both the problems of contact time and formation of coke through polyaromatic intermediates can be solved by employing a reactor design that quenches the reaction prior to solid carbon formation. This project involves an investigation of novel pyrolytic means of directly converting methane and natural gas into aromatic products with minimum formation of solid carbon. We propose the use of a reactor designed to rapidly quench the free-radical combustion reaction so as to maximize the yield of aromatics.

EXPERIMENTAL

The concept of the quench reactor is depicted in Figure 1. It consists of a double concentric quartz tube. Methane and a suitable diluent flow downwards in the outer tube, while water flows upwards in the inner tube to quench the reaction and limit the contact time. Figure 2 shows a schematic of the complete reaction system. The reactor tube is housed in a high temperature furnace having a 24-inch heated zone and capable of reaching 1540°C. Flows of methane and helium can be controlled between 80 and 2000 Scc/min using electronic mass flow controllers. The quench water is controlled using a needle valve and the flow measured with a calibrated rotameter. A solids trap at the outlet of the reactor traps any high molecular weight compounds that are formed.

Analysis is performed by on-line gas chromatography using a Varian 3400 GC equipped with an Alumina-GS Microbore capillary column. This arrangement is suitable for resolving all hydrocarbons of interest between methane and naphthalene.

THERMODYNAMIC CALCULATIONS

The thermal reactions of methane can be considered to follow mainly a stepwise dehydrogenation sequence, viz.:

$$2\,CH_4 \xrightarrow{-H_2} C_2H_6 \xrightarrow{-H_2} C_2H_4 \xrightarrow{-H_2} C_2H_2 \xrightarrow{-H_2} C$$

C_2 hydrocarbons are readily attacked by CH_3 radicals formed in the decomposition of methane forming higher hydrocarbon products. However, each of the four dehydrogenation steps indicated above is complex, involving a variety of free-radical and molecular intermediates. The final step from acetylene to carbon is believed to proceed through the formation of polyunsaturated and polyaromatic hydrocarbons followed by polymerization and loss of hydrogen. The hydrocarbon products which have been detected and identified in other studies are highly unsaturated and included ethylene, acetylene, propylene, propyne, butadiene, vinylacetylene, cyclopentadiene, benzene, toluene, naphthalene, methylnaphthalene, biphenyl, cyclopentadiene, biphenylene, and other less significant compounds such as styrene, indene, phenylacetylene.

Thermodynamic equilibrium calculations were carried out using PROCESS^{TM} Simulation Program in order to determine the maximum possible yields of various products from methane pyrolysis. Table 1 shows the thermodynamic product distribution of some products of interest allowing the reaction to proceed to the formation of solid carbon. In this case, mainly solid carbon (and hydrogen) is the reaction product. Some acetylene is formed in trace amounts at very high temperatures.

A similar calculation was carried out assuming that the reaction could be quenched at C_{10} aromatics, i.e., no higher hydrocarbons were allowed to form. Although all the products listed above were included in the thermodynamic calculation, the results revealed that only a limited number of products could be formed, at least in the range of temperature

studied. The major products identified are acetylene, benzene, and naphthalene. The minor products are ethylene, propylene, cyclopentadiene, methylnaphthalene and toluene. Vinylacetylene, butadiene, and propadiene were formed only in trace quantities.

The results of these thermodynamic equilibrium calculations are presented in Figures 3-7. Figure 3 gives the equilibrium methane conversion as a function of temperature. Figures 4 and 5 depict how the distribution of the major products vary with temperature, including and excluding hydrogen, respectively. Figure 6 similarly shows the product distribution for the minor products. Finally, Figure 7 represents the yields of the major products as a function of temperature.

These calculations show that the yields of benzene and naphthalene are highest in the temperature range between 1350 - 1550 K, with a maximum aromatic yield of ca. 45% (benzene + naphthalene) expected at about 1475 K (ca. 1200°C). Naphthalene is the most thermodynamically favored and stable hydrocarbon at these temperatures, while at much higher temperatures acetylene is the most favored product thermodynamically.

RESULTS AND DISCUSSION

Preliminary experiments have been performed at 900 and 1050°C in the absence of quench. Over 20 different products were identified in the reactor effluent by gas chromatography.

A summary of the results at 900°C are presented in Figure 8. Methane conversion at this temperature was low, i.e., less than 1%, but a number of products were identified. The principal product at this temperature was ethylene. Smaller amounts of propylene and benzene were also identified.

Figure 9 shows the conversion and selectivities for two separate runs at 1050°C and total methane flow rate of 100 Scc/minute. Methane conversions were 15 and 19%. The major products detected were benzene, acetylene, and ethylene. The benzene molar selectivity was ca. 50%, this is the equivalent of a benzene molar yield of ca. 7.5 - 10%. Figure 10 shows the effect of methane flow rate, i.e., space time, on the reaction. As would be expected, total methane conversion dropped with increasing flow rate. Conversion fell from 15% to 9% when the flow rate was increased from 100 to 200 Scc/minute. Changes in selectivities were also noted. Benzene selectivity decreased and ethylene selectivity

increased with increased flow rate. Flow rate seemed to have little effect in the acetylene selectivity, but this observation may be fortuitous. Other aromatics, including toluene and naphthalene were observed in small amounts at these conditions.

It is interesting that one of the major products observed was ethylene. This is contrary to the results of the thermodynamic calculation, indicating that the reaction is far from thermodynamic equilibrium under our reaction conditions. Similarly, the measured conversion was far below that predicted by thermodynamics for this temperature.

Reaction in the absence of a quench resulted in the formation of visible amounts of solid carbon, particularly at 1050°C. At this temperature, the formation of solids became evident after only a few minutes of reaction and, in one experiment, was sufficiently heavy to completely plug the reactor after only 100 minutes of operation. The resulting solid was not all carbon, as some of it was yellowish in color and was soluble in toluene. We are currently attempting to identify these materials.

REFERENCES

Agarwal, S.K., R.A. Migone, and Marcelin, G., (1989) Appl. Catal., 53, 71.

Brophy, J.H., (1987) UK Pat. Appl. 2,191,213.

Deryaguin, B. V., and Fedoseev, D. V., (1973) Carbon, 11, 299.

Driscoll, D.J., Martir, W., Wang, J.-X., and Lunsford, J.H., (1985) J. Am. Chem. Soc., 107, 58.

Friedman, N, Bovee, H.H., and Miller, S.L., (1970) J. Org. Chem., 35, 3230.

Keller, G.E. and Bhasin, M.M., (1982) J. Catal., 73, 9.

Khan, M. S., and Crynes, B. L., (1970) Ind. Eng. Chem., 62, 54.

King, D.L., Cusumano, J.A., and Garten, R.L., (1981) Catal. Rev.-Sci. Eng., 23, 233.

Leibson, I., Davenport, S.T., and Muenzier, M.H., (April 1987) Hydrocarbon Proc., 47.

Lieberman, M. L., and Noles, G. T., (1973), Chem. Vap. Deposition, Int. Conf., 4th, Boston, 19.

Makarov, K. I., and Pechik, V. K., (1974) Carbon, 12, 391.

Mimoun, H., Robine, A., Bonnaudet, S., and Cameron, C.J., (1989) Chem. Lett., 2185.

Murata, K, Sato, K., and Matsumoto, M., (1989) Jpn. Patent 1,085,321.

Oro, J., and Han, J., (1966) Science, 153, 1393.

Otsuka, K., Jinno, K. and Morikawa, A., (1986) J. Catal., 100, 353.

Pitchai, R. and Klier, K, (1986) Catal. Rev.-Sci. Eng., 28, 13.

Prado, G., and Lahaye, J., (1978) Chem. Phys. Carbon, 14, 167.

Quinian, M.A., Sancier, K.M., and McCarty, J.G., (1988) GRI Annual Report 5086-260-1328.

Sanchez, R.A., (1966) U.S. Patent 3,410,922.

Sperling, D. and DeLuchi, M.A., (1989) Energy, 14, 469.

Wiessermel, K. and Arpe, H., (1978) "Industrial Organic Chemistry", Verlag- Chemie, NY.